Space Science Reviews (2024) 221:3
https://doi.org/10.1007/s11214-024-01128-4

Seasonal and Short Timescale Changes on the Martian Surface: Multi-Spacecraft Perspectives

N. Thomas[1] · A. Pommerol[1] · E. Hauber[2] · G. Portyankina[2] · D. Tirsch[2] · F. Schmidt[3] · C. Cesar[1] · A. Valantinas[1,4] · V.T. Bickel[5] · G. Munaretto[6]

Received: 10 November 2023 / Accepted: 6 December 2024 / Published online: 19 December 2024

Abstract
The continued operation of missions such as Mars Express, Mars Reconnaissance Orbiter, and the ExoMars Trace Gas Orbiter has greatly enhanced our knowledge of seasonal processes on Mars. The most apparent evidence of the importance of seasons on Mars on the large scale is annual variation in the sizes of the Martian polar caps. However, high resolution imaging has also shown that seasonal forcing can lead to small-scale phenomena that are continuously changing the topography and the surface photometry. These phenomena often have no terrestrial analogue and involve complex interactions between seasonal ices, atmosphere, and substrate (surface and sub-surface). Although we now have better understanding of many of these processes (occasionally as a result of laboratory simulation), direct proof of some hypotheses remains elusive. We provide a brief review of the phenomena and list a series of open questions.

1 Introduction

Long duration missions to Mars over periods of greater than 1 Mars year provide the possibility to investigate processes that act on multiple timescales (diurnal, seasonal, annual and multi-annual). The observations by the imaging systems onboard Mars Express (MEx), the ExoMars Trace Gas Orbiter (TGO), and Mars Reconnaissance Orbiter (MRO) have been

✉ N. Thomas
nicolas.thomas@unibe.ch

1 Physikalisches Institut, Sidlerstr. 5, University of Bern, CH-3012, Bern, Switzerland

2 German Aerospace Center (DLR), Institute of Planetary Research, Rutherfordstr. 2, 12489, Berlin, Germany

3 Géosciences Paris-Saclay (GEOPS), Bâtiment 504, Rue du Belvédère, Campus Universitaire d'Orsay, 91405, Orsay Cedex, France

4 Present address: Brown University, Providence, RI, USA

5 Center for Space and Habitability, University of Bern, Gesellschaftsstrasse 6, CH-3012, Bern, Switzerland

6 INAF, Osservatorio Astronomico di Padova, Padova, and Department of Physics and Astronomy "G. Galilei", University of Padova, Padova, Italy

particularly important in identifying and tracking temporal changes and revealing recent geomorphological activity (Diniega et al. 2021). The spacecraft, however, have their own specific complementary strengths in this regard which lead to studies frequently using information from more than one spacecraft in addition to the somewhat more usual single-spacecraft multi-instrument investigations.

The orbit of NASA's MRO is around 250 km × 315 km and is Sun-synchronous passing over the equator at roughly 3:00 pm local time when over the dayside hemisphere (Zurek and Smrekar 2007). This orbit is ideal for high resolution imaging of local morphology. The High Resolution Imaging Science Experiment (HiRISE) takes full advantage of this with 25 cm/px imaging over a 6 km × ∼40 km swath providing a spatial resolution of a little over 50 cm (McEwen et al. 2007). It is a targeted imaging system where specific sites (targets) are selected in advance for acquisition during a two-week cycle. Investigations of seasonal processes with HiRISE are, by and large, local in nature. Multiple observations of a specific site during a season are constrained by the orbit repeat cycle but this is compensated by the ability of the spacecraft to roll up to ∼25° to view sites well away from the ground-track. Stereo observations can be acquired by using the roll of the spacecraft to obtain two images at different off-nadir angles. The spatial resolution of the resulting Digital Terrain Models (DTMs) is high but the illumination conditions vary between the acquisitions making stereo reconstruction at the highest resolution using photoclinometry challenging in some cases (see Kirk et al. 2021). The spacecraft also supports the Compact Reconnaissance Imaging Spectrometer for Mars (CRISM) which can perform high spatial resolution spectral identification of ices and minerals (Murchie et al. 2007). Both the Context Camera (CTX) and the Mars Color Imager (MARCI) provide context imaging for MRO (Malin et al. 2007) with MARCI being particularly important for studies of the seasonal evolution of the polar caps (e.g. Calvin et al. 2015, 2017).

The current orbit of the European Space Agency's (ESA) MEx is 298 km × 10,107 km with an orbital period of about 6.7 hours (Chicarro et al. 2004; see also Jaumann et al., this journal). Combined with the properties of the instruments, this results in a lower spatial resolution overview of surface changes but allows a higher observation frequency at different local times. Acquisitions from larger distances on the orbit (e.g. near apoapsis) provide a more synoptic view of seasonal processes. The High Resolution Stereo Camera (HRSC) takes advantage of its 175 mm focal length Apo-Tessar optical design (Neukum and Jaumann 2004) to acquire panchromatic and colour images processed to ground sampling distances (GSDs) between 12.5 m and 800 m as well as single pass stereo observations, allowing high quality DTM production at GSDs of up to ∼50 m/px (Gwinner et al. 2016; Kirk et al. 2020; Gwinner et al., this journal). The MEx payload also includes the Visual Monitoring Camera (VMC) which obtains synoptic observations are varying resolution but typically of the order of 10 km/px (Ormston et al. 2011). We note also the importance of the Observatoire pour la Minéralogie, l'Eau, les Glaces et l'Activité (OMEGA) instrument (Bibring et al. 2004a,b) which has played a key role in determining frost/ice composition and their seasonal spatio-temporal variability (Langevin et al. 2007; Langevin and Gondet 2020).

The orbit of ESA's TGO is roughly circular at 400 km above the surface with an inclination of 74° (Vago et al. 2015). The orbital period is nominally 1.96 hours and is not Sun-synchronous implying that observations can be acquired over the full range of local times. The Colour and Stereo Surface Imaging System (CaSSIS) is the imaging system onboard TGO (Thomas et al. 2017) and obtains high signal to noise, accurately calibrated, observations in 4 colours (NIR, RED, BLU, and PAN) at ∼4.6 m px^{-1} (11.36 μrad px^{-1}) (Thomas et al. 2017). The instrument includes a rotation mechanism allowing single pass stereo coverage in one overflight of a target. The orbit repeat cycle is, however, around 35 days and the maximum roll angle of the spacecraft has been restricted operationally to ±5°. As a result, the number of possibilities for repeat imaging coverage of a specific target is strongly latitude dependent and infrequent (approximately 6 times per Mars year) close to the equator leading to sparse data sets for detailed seasonal studies at lower latitudes. (The roll limit has recently been increased to ±7° per November 2023). The spacecraft also supports the Nadir and Occultation for Mars Discovery (NOMAD) instrument which can perform some spectral analysis of surface ices (Vandaele et al. 2018).

In this review, we shall emphasize the observations of diurnal, seasonal, and annual surface changes obtained by ESA's remote sensing missions, MEx and TGO while placing them in the context of the major contributions from other spacecraft (notably, NASA's MRO and Mars Global Surveyor). In the next section, we shall complete the introductory element by discussing the seasonal and diurnal CO_2 cycle on Mars. We shall then discuss the progress on studies of high latitude seasonal processes. The following section will describe studies of lower latitude processes resulting from condensation and sublimation of ices on seasonal and diurnal timescales. Other, possibly related, processes (including Recurring Slope Lineae, RSL) will also be covered here. The relatively recent evidence of the diurnal condensation cycle from imaging will also be presented as this provides an excellent example of the power of multi-spacecraft observations. Seasonal dust activity and its effect on the surface (see e.g. Geissler 2005) will be discussed in the penultimate section. Ripple and dune migration and landing site and impact changes are also briefly noted. A discussion of open questions that might form the basis for future investigations is also provided.

2 The Seasonal and Diurnal Condensation/Sublimation Cycle

The diurnal and seasonal processes producing changes on the surface are mostly related to atmosphere-surface interactions of various types. The most significant interaction is the condensation and sublimation cycle resulting from the orbit and obliquity of Mars (Leighton and Murray 1966). In this process, atmospheric CO_2 condenses on the unilluminated polar cap and its surroundings down to about 50° latitude during local winter to produce a layer of CO_2 ice on the surface that is of the order of 1 m thick (with reduced thickness at its margins). As spring arrives, this CO_2 ice layer sublimates progressively poleward (Acharya et al. 2024) until completely depleted thereby returning the CO_2 to the atmosphere and influencing the global atmospheric pressure (Hess et al. 1980; Haberle and Kahre 2010).

The surface atmospheric pressure is a balance between condensation at the unilluminated pole and sublimation at the illuminated pole and is driven by the obliquity and eccentricity of Mars' orbit combined with the radiative, reflectance, and topographic properties of the polar surfaces (see e.g. James et al. 1992 for a general description). These effects produce a >25% modulation of the surface atmospheric pressure over the Martian year (e.g. Hess et al. 1980; Zurek et al. 1992; Prettyman et al. 2009). The condensation and sublimation rates arise from an energy balance between the net absorbed solar energy (including volume absorption for semi-translucent ice), thermal radiative emission, and the temperature-dependent mass loss/gain resulting from the sublimation/condensation process combined with the latent heat. The mass exchange between the surface and the atmosphere in the energy balance equation can be approximated by the Hertz-Knudsen equation (e.g. Huebner et al. 2006; Zhang et al. 2017). The consequence of this energy balance is that, when in equilibrium, the temperatures of surfaces undergoing sublimation and condensation are constant while ice is present.

The control of the radiative behaviour of the Martian polar caps (and hence the energy input) by the CO_2 ice, H_2O ice, and dust properties was illustrated by Hansen (1997). Under current Martian pressures, CO_2 condenses at ∼148 K (see e.g. Hansen 2013 which also shows evidence for surface altitude dependence). Condensation temperatures are easily reached in the polar and circum-polar regions when no direct insolation is available, i.e. during polar night (Paige and Ingersoll 1985; Paige et al. 1994). As long as the surface stays at the condensation temperature, CO_2 readily deposits on it from the buffering, atmospheric, source. If extensive condensation reduces the pressure (locally or globally) the corresponding condensation temperature lowers reducing the deposition flux of CO_2. This creates a self-stabilizing system in which CO_2 on the surface stays at its condensation temperature allowing a sizable seasonal CO_2 layer to be created over many weeks. The periods of condensation vary in length with latitude and consequently the resulting ice layers have latitudinally-dependent thicknesses (Kelly et al. 2006).

Additional complications arise from the ability of CO_2 to deposit in different forms: the most common forms of CO_2 ice are translucent slabs (hereafter "slab ice") and granular CO_2 of various geometries (e.g. Portyankina et al. 2019). In the first case, when the ice becomes (semi-) transparent, energy is deposited on the substrate beneath the ice layer (Kieffer et al. 2006) or within the ice layer (i.e. volume absorption) as a consequence of contamination of the ice layer by sedimenting atmospheric aerosols (dust). A layer formed by granular CO_2 is much less dense and more porous. It probably contains inclusions of H_2O and dust particles more frequently. Hansen (2013) suggested that observations support a smoothly varying effective CO_2 grain size over the Mars seasonal polar cap.

Sublimation, condensation, and transport of other volatiles can also affect the properties of the polar ice layers and their formation/sublimation rates. H_2O, for example, participates in the seasonal atmosphere-surface exchange cycle, although its influence on the permanent surfaces is less evident because of its minimal concentration in the atmosphere (precipitable micrometers). The seasonal cycle of atmospheric water vapour has been studied for many years (examples of global studies include Fedorova et al. 2004; Maltagliati et al. 2011 and Pankine 2022 while local studies include that of Khayat et al. 2022) and its presence and layering of water ice in the permanent polar caps has been described in numerous publications (e.g. Bibring et al. 2004a,b; Seu et al. 2007; Putzig et al. 2009; Orosei et al., this journal). Its role in the sublimation/condensation of the seasonal caps is discussed further below. In addition, the relative abundance of light non-condensable species (Ar, N_2, CO, etc.) increases in the atmosphere when CO_2 condenses, providing a barrier to CO_2 transport. This results in a decrease of the CO_2 partial pressure and depressing the local frost point temperature by between 0-4 K (Piqueux et al. 2023).

The CO_2 cycle itself is evident in imaging observations in the seasonal growth and retreat of the Martian polar caps and how the caps respond to the changing illumination (Fig. 1). The physical processes associated with the condensation and, particularly, the sublimation are themselves interesting because there is no Earth analogue of such processes. However, the cycle also influences the substrate resulting in year-on-year topographic changes. In addition, localised condensation of CO_2 on surfaces that are equatorward of the ice sheet but illuminated poorly or unilluminated in winter as a consequence of topographic relief can also modify that topography locally through, for example, mass wasting. The effects of these processes are typically over smaller scales (at the scale of the topography – 100 m scales) and consequently moderate to high resolution imaging, ideally combined with colour, is needed to identify them. However, their influence on the Martian landscape should not be underestimated and indeed many of these effects can result in simplified access to older sub-surface materials.

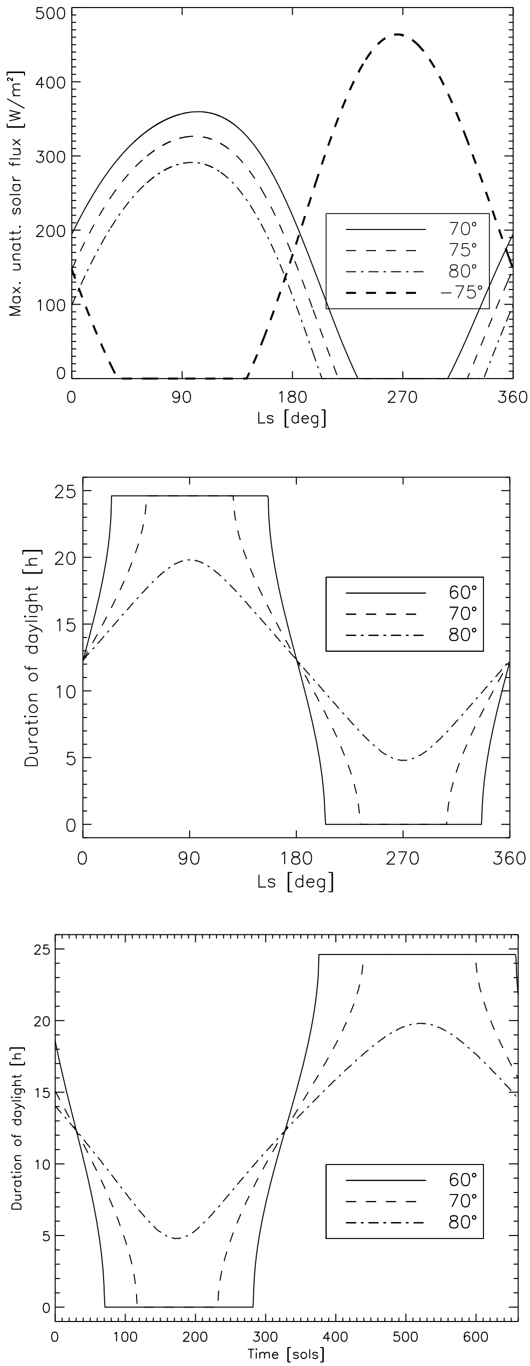

Fig. 1 Top: The variation of the peak solar flux (midday) on a flat surface at different latitudes assuming no atmospheric attenuation. The values are plotted against season (Ls). Three northern latitudes are shown (70°N – solid, 75°N – dashed, 80°N – dot-dash) and one southern latitude (75°S – solid, thick). Middle: The duration of daylight at 3 northern latitudes (60°N, 70°N, 80°N) on a flat unshadowed surface expressed again Ls. Bottom: As middle but expressed against time (linearly). Note the difference between northern and southern summer in the top panel and the continuous illumination (darkness) seen in the lower panels

3 The Seasonal Polar Caps

3.1 Larger-Scale Behaviour

While albedo estimates from Earth informed early models of seasonal processes involving CO_2 sublimation/condensation (Leighton and Murray 1966), orbital mapping has considerably improved our knowledge of the reflectivity of icy units throughout the seasons and the broader range of wavelengths accessible in space have allowed refinement of their distribution, composition and properties and observation over a range of wavelengths (e.g. Oliva et al. 2022). Naively, one might expect the longer-term stability of the Martian orbit and rotation to result in a highly stable annual cycle. Indeed, observations at thermal infrared wavelengths by Thermal Emission Spectrometer (TES) and MCS (Piqueux et al. 2015) have shown that growth and retreat of the northern seasonal cap is symmetrical around the pole and extremely repeatable from year to year. Even extensive dust storm events do not significantly alter the deposition pattern, although the recession of the cap is accelerated. The southern cap, however, exhibits different behaviour. It is asymmetric (cf. Giuranna et al. 2008; see also Giuranna et al. 2007) because of regional topographic control (i.e. the Hellas and Argyre basins have a significant effect) as well as showing year-to-year variability (Piqueux et al. 2015) especially during retreat.

The seasonal thickness changes of the polar caps were studied by Aharonson et al. (2004) using the Mars Observer Laser Altimeter (MOLA). The most recent work has been by Xiao et al. (2022a, 2022b) who indicate that the maximum level over the Residual North Polar Cap is just 1.3 m as compared to 2.5 m over the south pole. Exceptionally, the maximum ice depth in the dune fields of Olympia Undae can be up to 3.8 m. However, some unresolved issues on the ice thickness variations with time remain.

The optical reflectances of the icy layers found at high latitude control their seasonal and long-term evolution through absorption and reflection of sunlight. The reflectance can be diagnostic of layer composition (CO_2 vs. H_2O) and physical properties (grain size, roughness, etc.). Fresh crystalline CO_2 frost is extremely bright in visible wavelengths, while slab ice is translucent and the surface may appear to a visible imager as unfrosted. Hence, visible imagers provide indicators for presence of the surface ice but need to be combined with either temperature measurements or spectral data to confirm presence and/or absence of either CO_2 or H_2O ice. Detection of mixtures is even more problematic because the spectral signature of H_2O is significantly stronger than that of CO_2 and thus easily masks surficial CO_2 deposits even when H_2O layers are only mm thick. Establishing ice properties is a primary objective of many orbital missions to Mars. Mars Express, with its large variety of observation conditions and wide suite of instruments covering a broad wavelength range has provided unprecedented views of the Martian high latitudes in different seasons and various times of day. These datasets were instrumental in refining existing scenarios and identifying more detailed seasonal processes involving ices occurring at high latitudes.

From the early mapping observation of the permanent caps on the Martian poles, the northern cap was believed to be mainly composed of water ice, whereas the southern cap was thought to be CO_2. Early in the mission, hyperspectral images obtained by OMEGA (Observatoire pour la Mineralogie, l'Eau, les Glaces et l'Activite) revealed exposures of water ice in the scarps of the south polar layered deposits (Bibring et al. 2004a,b; Douté et al. 2007). The OMEGA dataset has been extensively used to better characterize the seasonal ice layer throughout its sublimation from the end of winter to summer (e.g. Appéré et al. 2011; Langevin et al. 2006; Schmidt et al. 2010). It has allowed the monitoring of surficial CO_2, differentiated it from H_2O, and, to some extent, defined its physical form.

After emerging from polar night, the overall reflectance of the seasonal deposits evolves significantly throughout spring with a general brightening around and after spring equinox interpreted as the result of a decrease of the grain size. A subsequent decrease of reflectance towards summer occurs as the ice sublimates and patches of bare substrate appear. Comparing the observed spring evolution of the southern seasonal cap with results from global circulation models, Schmidt et al. (2009) concluded that it is the surface albedo of the ice deposits which controls the speed of their recession. There are, however, longitudinal differences evident which may not be albedo related.

For example, in the south, TES observations (Kieffer et al. 2000) led to the detection and definition of a "cryptic" region. The term "cryptic" was coined to express the counter-intuitive property of the surface – namely that a dark (at visible wavelengths) surface was also observed to be cold contrary to that expected from a simplified thermal balance. This region has been shown to modify the seasonal cap retreat. OMEGA specifically observed CO_2 to retreat faster in the "anti-cryptic" area in the latter part of southern spring. Also in the south, OMEGA observed the CO_2 top-surface to be spatially heterogeneous and evolving with time (Schmidt et al. 2009). Observations at the end of winter revealed large grains of CO_2 over the entire southern seasonal cap, consistent with the transmission of sunlight through CO_2 slab ice to the substrate as required by Kieffer's hypothesis (Kieffer 2000, 2007; Kieffer et al. 2006; Langevin et al. 2007; see below). In spring, however, the low albedo of the "cryptic region" is consistent with dust in the surface layer rather than a translucent slab.

Contrary to the southern hemisphere, water plays a key role in the spring evolution of the northern seasonal cap. In the north, Appéré et al. (2011) observed that during winter, the CO_2-rich condensates are initially transparent and could be in slab form. The annulus surrounding thick slab deposits consist of CO_2 with H_2O trapped in it, that during the sublimation season gets gradually released into the atmosphere. Interestingly, this water gets cold-trapped on the retreating CO_2 and "migrates" towards the pole during spring.

Despite its low abundance within the CO_2 ice layer in winter, H_2O appears to mask totally the spectral signature of CO_2 from the surface over a large annulus in late spring (Appéré et al. 2011). This evolution is associated with a substantial brightening of the seasonal cap in mid-spring.

Two mechanisms have been proposed to explain this apparent disappearance of surficial CO_2: cold trapping of water vapour sublimated at lower latitude by CO_2 ice or local accumulation at the surface of H_2O ice particles previously embedded in the CO_2 layer and released by its sublimation.

Pommerol et al. (2011) used a combination of spectral and visible data to investigate the evolution of seasonal ice layer during its spring retreat on a regional scale. They reported that the reflectance of the top surface at several locations in the southern polar regions increases between L_s=200° and 240°. Surprisingly, there was no significant correlation with water absorption band strength and only a weak correlation with CO_2 absorption band strength in CRISM data. Pommerol et al. (2013) reported a similar brightening event in the northern polar regions between L_s= 0° and 40°. Other brightening events were independently detected by the MARCI and OMEGA instruments (Calvin et al. 2015). The high spatial resolution data of HiRISE and CRISM revealed that local winds cause the removal of the H_2O veneer from the surface of the CO_2 ice layer and are responsible for the sudden reappearance of the CO_2 spectral signatures in late spring (Pommerol et al. 2013).

The Martian water cycle is tightly coupled to the polar regions (Alsaeed and Hayne 2022) and water ice particles may act as condensation nuclei to facilitate CO_2 snowfall (Määttänen et al. 2022). Kuzmin et al. (2012), using TES and OMEGA data, confirmed that the seasonal permafrost exposed by the retreating northern polar cap is actively involved today in the condensation and sublimation processes in the modern water cycle. Modelling (Alsaeed and Hayne 2022) suggests that 10^{10} kg of water can participate in this cycle.

Gary-Bicas et al. (2020) show that snowfall and dust loading are important in modelling the CO_2 cycle because they influence the composition and emissivity of the seasonal caps. Such models have, for example, indicated that an increase in dust deposition on the caps during and after major dust storms can slow the retreat of the southern seasonal cap in spring although the effects on the northern cap retreat rate are less profound and minimal because the major influence occurs at the highest latitudes (>80°N) (Zhao et al. 2021). On the other hand, this is somewhat counter-intuitive because dust deposition should increase solar insolation energy deposition in spring. However, the dust may become thick enough to provide a protective layer, reducing the sublimation rate.

In conclusion, it is often necessary to invoke relatively complex processes to explain the larger scale phenomena and a complex thermophysical interplay between the volatiles, the substrate, and non-volatile aerosols is at work.

3.2 Araneiforms and Other Erosional Processes

Araneiforms are converging systems of branching troughs exhibiting fractal properties (Portyankina et al. 2020). They are believed to be the result of repeated CO_2 jet eruptions produced in the frame of Kieffer's model process. When these eruptions happen at the same location over hundreds and maybe thousands of years, the small but continuous erosion acting on the substrate shapes it into the troughs and systems of troughs that we call araneiforms. Araneiform fields are among the most active areas in the martian southern polar regions. Because of their unique morphology (Fig. 2) and gaps in our understanding of the processes forming them, araneiforms are being extensively monitored by different instruments: cameras, spectrometers, thermal imagers, etc. One of the goals has been to characterize the rates of erosion by the cold CO_2 jets because, so far, there has been no direct observation of changes in any of the well-developed araneiforms (McKeown et al. 2021). This might be the result of the technical constraints (e.g. resolution) of such observations or because, under the current conditions, araneiforms are dormant.

On the other hand, strikingly similar features but on a smaller scale have been observed to appear and evolve under the current climate. Dendritic troughs were found by Portyankina et al. (2017) in overlapping HiRISE images of inter-crater dune fields. Dendritic troughs are morphologically similar to furrows which are small-scale sinuous channels eroded by sub-ice gas flow, usually on dunes. They are of the same spatial scale (width of several metres, lengths of tens to hundreds of metres). However, a distinction is made between these two types of erosion features because furrows are transient while dendritic troughs remain visible for more than one Mars year. Dendritic troughs also develop into more complex patterns from year to year – a trait that furrows fail to exhibit because they are erased every summer by the movement of the dune material they are carved into. The appearance and evolution of dendritic troughs shows that processes described by Kieffer's model can indeed modify the permanent substrate and, given enough time, could create larger araneiform fields. Modelling of the structures has been presented by Portyankina et al. (2019) by analogy with drainage networks using a strictly mathematical model for pattern formation that was first introduced for a completely different application by Witten and Sander (1983).

If we assume that the araneiform production process has been active over much of the last obliquity-eccentricity cycle (Laskar et al. 2002) and that the structures are metre-sized in depth then it is apparent that erosion rates of only microns per Martian year would be needed to reproduce the observations.

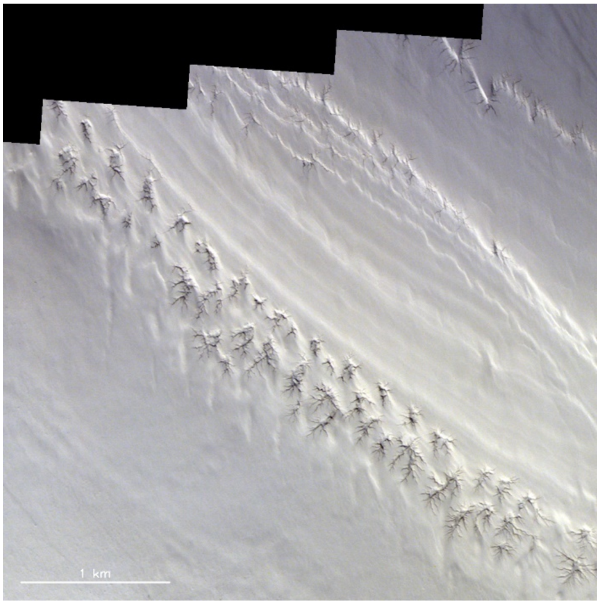

Fig. 2 Araneiforms on layered terrain seen by CaSSIS (MY35_014028_278_0) on 14 Jan. 2021 at 11:04:32. Long. 196.8°E Lat. 72.7°S. (All acquisition times and image centres for CaSSIS observations shown herein are collected in Table 1). Evidence of activity is apparent in the form of dark deposits near the centres of some of the “spiders”. Credit: ESA/TGO/CaSSIS CC BY-SA 3.0 IGO

Table 1 Acquisition times and centre coordinates of CaSSIS images shown in this work

Image Id	Figure	Time of acquisition	East longitude [°]	Latitude [°]
MY35_014028_278_0	2	2021-01-14T11:04:31.910	196.768	-72.693
MY34_002139_276_0	3	2018-05-17T04:37:09.640	265.012	-72.69
MY36_019238_263_3	3	2022-03-17T01:16:15.038	167.273	-73.561
MY34_002199_302_1	4	2018-05-22T02:36:30.651	12.664	-54.432
MY35_013770_237_0	4	2020-12-24T07:51:04.671	12.798	-54.348
MY36_018110_237_0	4	2021-12-14T16:28:19.145	12.896	-54.406
MY35_013935_280_0	7	2021-01-06T20:19:08.094	10.257	-72.123
MY35_011076_242_0	8	2020-05-17T17:50:27.961	257.475	-57.331
MY34_004583_256_0	9	2018-12-03T04:47:53.588	1.326	-68.418
MY36_018111_253_0	9	2021-12-14T18:31:35.659	1.292	-68.36
MY35_014188_345_0	11	2021-01-27T13:51:49.665	294.435	-12.996
MY35_011368_288_0	13	2020-06-10T15:54:53.325	195.443	-66.496
MY36_015964_025_0	14	2021-06-21T22:10:14.399	28.5	23.534
MY37_024386_022_3	14	2023-05-12T12:22:52.377	33.976	20.753
MY34_005400_153_0	15	2019-02-08T00:54:57.500	57.048	26.067
MY37_025092_162_0	17	2023-07-09T08:30:56.387	283.8	17.531

3.3 Kieffer’s Basal Sublimation Hypothesis and Observational Constraints

Kieffer’s basal sublimation hypothesis emerged from the observation of araneiforms (spider-like morphologies) in substrates and dark fans superposed on ice-covered polar surfaces in spring by the MOC imager. It provides a theoretical framework for the formation mechanism of such features from the interaction between the Martian surface and the seasonal CO_2

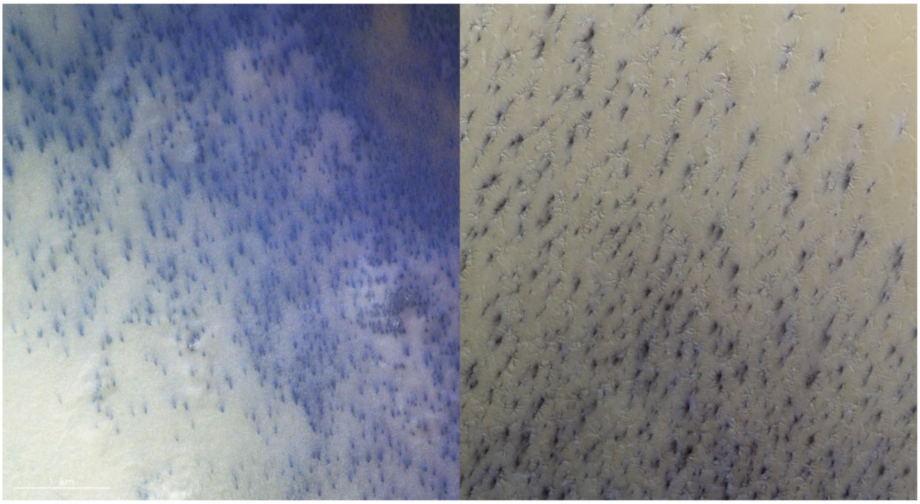

Fig. 3 Images of fan-like deposits on an ice-covered substrate seen by the CaSSIS imager on TGO. Left: Sub-frame of image MY34_002139_276_0. Right: Sub-frame of image MY36_019238_263_3. The image to the right shows araneiforms with associated fan-like activity. Credit: ESA/TGO/CaSSIS CC BY-SA 3.0 IGO

ice layer (Kieffer 2000). Figure 3 shows CaSSIS images (acquired at a scale of 4.5 m/px) of dark fans with Fig. 3 (right) showing relationship to araneiforms. Kieffer's conceptual model suggests that high incidence angle spring sunlight passes through translucent seasonal CO_2 slab ice and is absorbed by the underlying regolith. Thermal emission is ineffective at cooling the substrate because CO_2 ice is opaque at thermal IR wavelengths (13-18 μm; Hansen 1997). Hence, the substrate warms and causes the surrounding ice to sublime. The ice is essentially a conformal coating and traps the gas at the interface. Such behaviour has been observed in the laboratory (Portyankina et al. 2019). As the pressure builds up, the slab cracks at weak points within the ice, expelling gas through the created openings. The sub-slab gas flow erodes the substrate producing dendritic troughs around the vent. The eroded particles from the substrate are carried by the flow through the vent and deposited onto the ice layer surface, forming dark spots and fans of varying shape. The shapes are influenced by the local winds and topography (Piqueux et al. 2003; Kieffer et al. 2006; Thomas et al. 2011). Multiple events through a single vent are inferred from the fact that multiple deposition fans can be seen in different orientations in many cases (Thomas et al. 2010) – also indicating variable wind direction. Wind variations are believed to be responsible for the shapes of fan deposits, especially their lengths and opening angles: the stronger near-surface winds are, the longer will be fan deposit, and if the wind shifts while the jet is active, the regolith material will deposit over larger opening angles. Aye et al. (2019) have used a database generated from a citizen science project to determine prevailing wind directions using this phenomenon.

Models of gas flow through the vent have been produced (Thomas et al. 2010, 2011 which constrain the maximum height expected from quasi-explosive venting (typically 150 m) and also from continuous venting arising from long-duration basal sublimation. Deposition patterns arising from particulates in the flow have also been modelled with good, albeit unsurprising, agreement with observation.

Since its introduction, this well-accepted conceptual model has been adapted and refined using additional orbital data (eg. Kieffer et al. 2006; Piqueux and Christensen 2008; Cesar et al. 2022). A wide range of feature morphologies have been observed (e.g. Hansen et al. 2010 and Hao et al. 2019 for araneiforms) while time variability of spots (non-fan-like but more rounded, dark deposits) has been discussed by Cesar et al. (2022).

It needs to be noted, however, that the act of venting has never been unambiguously observed from orbit. Thomas et al. (2010) showed the presence of a long narrow fan that several days later had completely disappeared. These were however single shot images and, with no stereo confirmation (as was possible in the case of a similar process on Triton; Kirk et al. 1990), alternative explanations to geyser-like activity cannot be ruled out. Through experimental studies, the transport of substrate material via a conduit of a slab of CO_2 ice has been shown to be effective and correlates well with the core of dendritic patterns similar to the ones observed on Mars (McKeown et al. 2017, 2021; de Villiers et al. 2012). Several hypotheses have been proposed for the lack of data (Hansen et al. (2019, 2020) and Thomas et al. (2011)):

1- The jets could be active at local times at which many missions do not fly over the polar regions due to their sun- or quasi sun-synchronous orbits (MGS and MRO for which MOC and HiRISE imagers are examples). Calculation of accumulated solar irradiation on inclined surfaces located at high latitudes suggests that during early spring eruptions are most likely to happen in the early afternoon. The time of eruptions then shifts towards morning together with progressively earlier sunrises. TGO (CaSSIS imager) and Tianwen-1 Orbiter (HiRIC and MoRIC imagers) have solar asynchronous orbits which provide variability in the local time of observations of high latitude areas but no positive detection of a jet in action has yet been obtained. HRSC on MEx may not have sufficient spatial resolution.

2- The jets, composed of CO_2 gas and fine particles (μm- to mm-sized) from the eroded substrate, may not be detectable from orbit because of the small optical depth with respect to the surrounding illuminated surfaces. (Put another way, the imaging instruments do not have sufficient signal to noise to detect them.) This could be the result of low particle production rates or possibly be connected to the vent morphology.

3- The deposits associated with jet activity may come from low-intensity venting of the excess basal pressure possibly after an initial quasi-explosive event. Hence they may be small and therefore difficult to identify from orbit.

4- Activity durations may be short - possibly a few minutes to hours at most and, hence, the opportunity and feasibility of observing such phenomena is highly reduced. (Put another way, we have been unlucky!)

5- There could also be an element of misinterpretation. The dust in the jets could be relatively bright because of scattering with maximum brightness close to the vent. This is then misinterpreted as indicating that a bright surface (associated with topography) is being illuminated by the Sun.

Well-correlated atmospheric features have been detected (e.g. Figs. 17, 19, 20 of Cesar et al. 2022) in a few instances near seasonal features which may be indicative of atmospheric cooling arising from the expansion of the jet into the ambient atmosphere. A larger dataset, including study of the local atmospheric temperature profile, is required to provide sufficient confidence in this explanation of the observational data.

4 Ice- and Frost-Related Dune Activity

Seasonal activities on Martian dunes can be of various natures. These include frost deposition and defrosting causing dark spots, dark streaks as well as dune gullies and general mass wasting. The most prominent seasonal changes on dunes are caused by the condensation and sublimation of CO_2 frost, a process that depends strongly on the course of the Martian seasons. The activity of dust devils and the aeolian migration of ripples and dune surfaces can also be subject to a seasonal cycle and are discussed below.

4.1 Mass Wasting

CO_2 sublimation-driven mass wasting processes on dune slip faces in the north polar region has been presented for the first time in a HiRISE-based study by Hansen et al. (2011). They showed that grain flow on dune slip faces causing new alcoves and gullies occurred within one Martian year. The volume of the moved material has been estimated to be in the range of tens of cubic metres. The downslope transport of material results in the extension of preexisting or the formation of new aprons on the dune's slip face foot, with sizes in the range of several metres length and tens of meters width.

The initial hypothesis was that the mass wasting is primarily caused by destabilization of slip faces resulting from sublimation of CO_2 frost. However, an analysis by Horgan and Bell (2012) of dunes in the north polar erg showed that new alcoves and avalanches at Tenius Cavus are already present under a layer CO_2 frost prior to sublimation in early spring, implying that they formed before the frost was deposited on the dune surfaces. Instead, the authors suggest that the formation of the observed new alcoves occurred sometime during middle to late summer. This timing of the mass wasting processes is rather consistent with a formation primarily caused by aeolian processes, which is supported by the orientation of the alcoves consistent with current wind directions (Horgan and Bell 2012). The initial deposition of CO_2 in winter might also act as a trigger.

4.2 Spots and Streaks

Defrosting sublimation spots typically start in the local late winter through to spring as a result of the CO_2 jetting process described above. This process is prevalent but not limited to polar regions and high latitudes, having also been observed at mid- to lower latitudes (e.g., Kieffer et al. 2006; Kieffer 2007; Piqueux and Christensen 2008; Gardin et al. 2010; Hansen et al. 2010; Portyankina et al. 2010; Thomas et al. 2010; Piqueux et al. 2016).

In a recent study by Rangarajan et al. (2023), different stages of defrosting on a dune field in Aonia Terra (65.67°S; 257.02°E) have been observed with CaSSIS colour infrared composites. The spring-time NIR-PAN-BLU composite of CaSSIS filter images nicely shows the frost layer on the dunes in a distinctive pale-blue colour, interrupted by numerous circular dark spots of varying sizes. The presence of ice was confirmed with the ICE-ATM spectral parameter (Tornabene et al. 2017) that helps distinguish between bright ice and frost from other bright features such as clouds or dust devil tracks. The dark spots possess lower ICE-ATM values in the spring image confirming the sublimation of ice at these locations. For comparison, a summer-time composite of the same dune field displays the aeolian deposit with its typical low albedo and the ice parameter map confirms the complete sublimation and disappearance of the frost (Rangarajan et al. 2023).

The most studied dune field with gullies outside from the polar region is probably the Russell crater dune field in Noachis Terra (e.g., Mangold et al. 2003; Reiss and Jaumann 2003; Diniega et al. 2010; Gardin et al. 2010; Reiss et al. 2010; Jouannic et al. 2012; Douté et al. 2015; Dinwiddie and Titus 2021; Fig. 4). Observations of seasonal activity led to the determination of a defrosting sequence with dark spots appearing in the middle winter over the frost covered south-west facing scarp, growing and grading into dark streaks over the

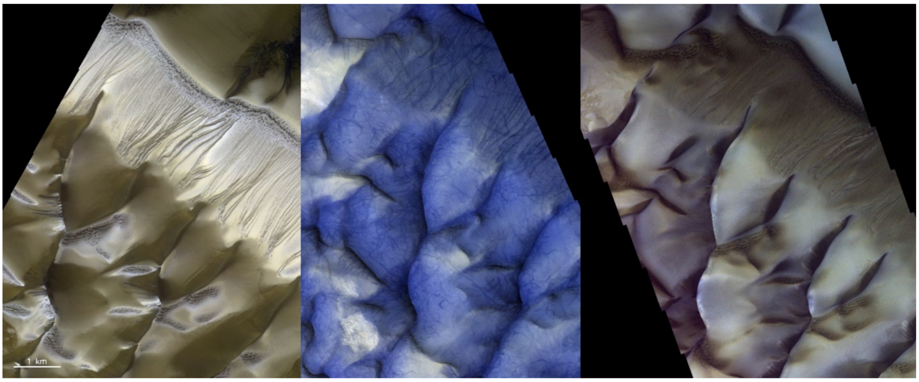

Fig. 4 Part of the Russell crater dunes (12.5° E, 54.5° S) acquired by CaSSIS at different times of the Martian year. Left: MY34_002199_302_1, Ls=179.7°, Local time=14:38:57. Centre: MY35_013770_237_0, Ls=336.6°, Local time=10:09:09 Right: MY36_018110_237_0, Ls=141.9°, Local time=07:55:58) A 1 km scale bar is at the bottom left. Credit: ESA/TGO/CaSSIS CC BY-SA 3.0 IGO

course of the season, which then extend downslope as dark flows with decreasing activity as early spring approaches (e.g., Gardin et al. 2010; Douté et al. 2015). The flow features on this megadune are 1 to 2 m wide and 50 to 100 m long and expand episodically with a velocity between 2 to 4 m/s. Analyses of CRISM data revealed that the defrosting process is not continuous as springtime data shows refrosting under the brink of the dune field.

It has been suggested that the linear gullies on this megadune were carved by liquid water bearing debris flows (Mangold et al. 2003; Reiss and Jaumann 2003; Jouannic et al. 2012) implying a formation during warmer climatic episodes. Although the nature of these dark flows argues for erosional processes, a direct connection between the linear gullies on the Russell crater megadune and the dark flows has not been established by Gardin et al. (2010).

Direct links between dune gully activity and CO_2 frost accumulation have been presented by Diniega et al. (2010) for several dune fields in the southern midlatitudes (including Russell crater) by means of HiRISE, MOC and CTX images as well as HRSC topography data. Their analyses showed present-day dune gully activity was evident in significant apron, channel and alcove modification over the course of three Martian years. The main activity was constrained to the winter season, implying a seasonality of this process and supporting the hypothesis that CO_2 frost accumulation is the main driver for the (re-)activation of the studied dune gullies. Similar processes have been reported by Diniega et al. (2019) for dune gullies in the north polar region with major activity phases at the local autumn and winter.

Larger dark dune spots and low-albedo slope structures of sizes between 20 and 200 meters on a dune field in the southern polar region have been discussed in an earlier study by Horváth et al. (2009) by using HRSC, MOC, and HiRISE data. Processes involving dry mass movement, liquid CO_2, liquid water, and gas-phase CO_2 have been discussed as possible formation mechanisms of the dark-albedo features. The authors report the occurrence of the dark dune spots between the end of winter and beginning of summer whereas the dark slope features likewise appeared in spring in subsequent Martian years confirming the seasonal nature of these phenomena. According to this study, the dark dune spots fit well with the model of escaping CO_2 gas jets, which is the current interpretation of such seasonal dune features. Here, either the combination with wind transporting the dark dune material away from the spots or the dust ejected by the jets falling back onto the surface near the spot (Kieffer et al. 2006) results in the often fan-shaped structure of these features. For the dark slope structures, Horváth et al. (2009) favor a hypothesis including liquid water because the seepage-like morphologies of the confined streaks suggest the action of some fluid-like material. Following this hypothesis, increasing solar insolation causes a growing liquid film on the sand grains under a water ice frost cover which causes seepage flow until the dunes are defrosted (Horváth et al. 2009). However, the authors acknowledge that the greatest problem of this hypothesis is the maintenance of liquid water on Mars and summarize that none of the discussed models give a satisfying interpretation of all features presented.

The flow of liquid brines has also been proposed as an explanation for fast growing dark streaks on dunes at the high northern latitudes, with growing velocities between 0.3 to 7 m/day and at temperatures between 150 K and 180 K (Kereszturi et al. 2008, 2009a,b, 2010). However, Hansen et al. (2011) argues that liquid salt brines require temperatures greater than 200 K and a frost-free surface, which is not compatible with the observations of the dark streaks in early spring when the surface temperature is at CO_2 sublimation point. Chevrier et al. (2022) have performed laboratory analyses that show that liquid brines of plausible composition are unstable under present-day Martian conditions and are unlikely to contribute to surface geomorphological activity, such as Recurring Slope Lineae (RSL; see below).

5 North-South Dichotomies in Seasonal Polar Processes

At the first glance, northern and southern seasonal processes are similar: in both hemispheres they are essentially linked to the global CO_2 cycle (with minor contamination of H_2O and modulation by dust events), predominantly driven by insolation, and respond to dust contamination by atmospheric transport. Visually, morphological representations of the seasonal processes have strong similarities: both seasonal polar caps wax and wane, dark fans, spots, and blotches appear and merge, dark dust avalanches creep down the dune slopes, scarps in the polar layered deposits get eroded by repeated avalanches, etc. However, there are significant differences between the hemispheres which are evident in seasonal processes (Thomas et al. 2000). From simple orbital considerations, winter in the south is longer than in the north providing more time to accumulate thicker seasonal CO_2 layers in the southern polar regions. The onset of spring and change in insolation is more rapid in the south with larger thermal gradients over time, across latitudes, and, especially, on equator-facing slopes. The mean elevation of the southern hemisphere is higher, leading to lower pressure and lower phase transition temperatures. Differences in topographic height also influence atmospheric dynamics and results in different wind regimes and H_2O content over the two hemispheres.

It was noted above that, on the medium to large scales, the seasonal behaviour differs between the hemispheres. Here we discuss several observed differences of the small-scale seasonal behaviour. These differences are harder to spot not only because of the obvious difficulty of consistently observing small-scale features but also because, at these scales, latitudinal, regional and inter-annual variations might be as influential, if not more so, than the hemispheric differences.

The spatial scale of fans and blotches that are produced by basal sublimation of the seasonal CO_2 ice layer differ between north and south. In the north, these processes predominantly occur on the circum-polar dunes, while in the south they are mainly (but not exclusively) on araneiform-type terrains. The scales of the produced fans and blotches are smaller in the north compared to south (Hansen et al. 2011). This implies that the process of CO_2 eruption may be less violent and less energetic in the north suggesting that the northern

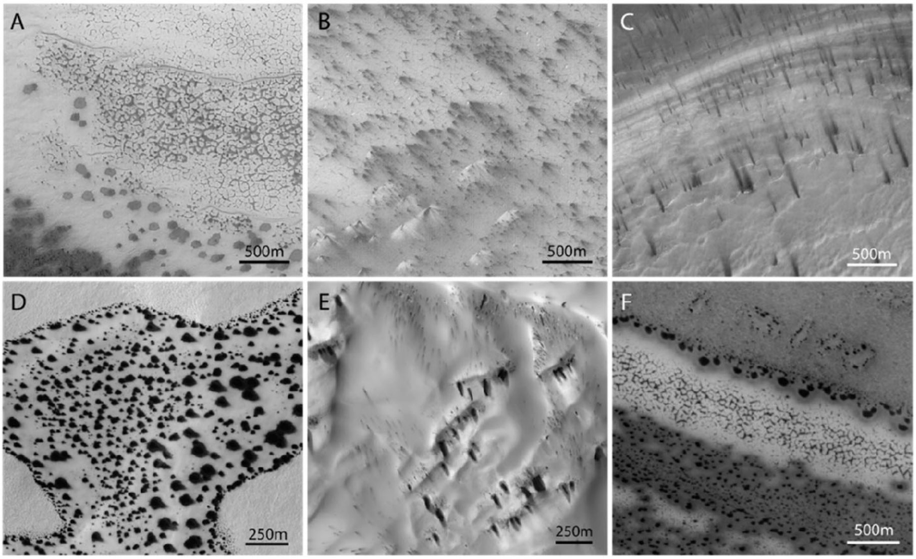

Fig. 5 Examples of MOC (top row) and HiRISE (bottom row) images of dark spots and fans in the southern polar area of Mars. Each panel information is reported in Table 2 indicating the corresponding ID, acquisition time, coordinates, and Martian parameters. Image credits: NASA/JPL/MSSS & NASA/JPL-Caltech/UArizona

Table 2 Table of MOC and HIRISE image acquisition information for Fig. 5

	Images information									
	Panel	ID	Acquisition Date/Time	Latitude	Longitude	Season	Ls	Sol	MM	MY
Spots & Fans	A	R0601729	2003-06-27T03:02:01.79	80.4°S	200.2°W	Southern Spring	210.6°	423	8	26
	B	R0600982	2003-06-19T02:44:28.40	87.3°S	192.4°W	Southern Spring	205.8°	415	7	26
	C	S0602060	2005-05-22T22:56:25.47	84.7°S	259.3°W	Southern Spring	216.1°	432	8	27
	D	ESP_011605_1170	2009-01-16T18:13:53.444	62.5°S	53.3°E	Southern Spring	192.6°	394	7	29
	E	ESP_029614_1105	2012-11-20T00:34:44.720	69.5°S	153.4°E	Southern Spring	210.1°	422	8	31
	F	ESP_038024_1005	2014-09-06T08:29:56.712	79.6°S	234.9°E	Southern Spring	191.3°	391	7	32

seasonal changes are more subdued. This may be simply explained by the winter CO_2 ice layer being thinner in the north although this relationship is not proven.

Furrows are more common in the north compared to south. This is probably the result of dune material in the north being less consolidated. The hint that dunes are more mobile and thus less consolidated in the north comes from calculations of fluxes of moved material over several martian years (Chojnacki et al. 2022). Southern dunes show less mobility than northern dunes.

Another detectable difference between the hemispheres is the presence of araneiforms only in the southern hemisphere. While araneiforms themselves are not seasonal features, they are believed to be formed by seasonal processes. It is unclear why their formation would be limited to the southern hemisphere.

5.1 Seasonal Scarp Erosion

Steep fractured scarps are prominent along the margins of Planum Boreum (near 84°N, 236°E) in the northern hemisphere (Herkenhoff et al. 2007). These scarps are up to 700 m high and have slopes of up to 70°. They expose two geological units - the North Polar Layered Deposits (NPLD) (Byrne 2009; Tanaka and Scott 1987) and the sandier Basal Unit

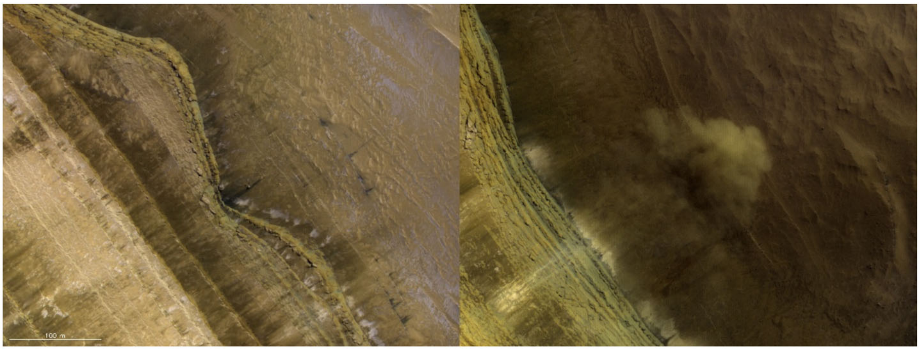

Fig. 6 Two HiRISE images of northern polar scarps. No map projection has been applied but a 100 metre scalebar has been placed bottom left. It is approximate. Left: ESP_033766_2650 showing boulders at the foot of the scarp and streaks of various brightness extending downslope. Right: Image ESP_025010_2650 contains one of the more well-known avalanches seen in progress by HiRISE. Note the cloud of debris and the bright material at the base of the scarp. Credit: NASA/JPL-Caltech/UArizona

(BU) (Byrne and Murray 2002; Herkenhoff et al. 2007; Fanara et al. 2020a). The steepness of slopes combined with their location at high latitudes means that the slopes are at near orthogonal illumination, particularly in spring. Local high solar flux results in rapid sublimation of seasonal CO_2 layer in spring (Hansen et al. 2013; Piqueux et al. 2015). On-going mass wasting, in the form of avalanches and ice block falls, has been recorded (Russell et al. 2008, 2012) with HiRISE (Fig. 6 right) and is clearly seasonally dependent. The ice blocks resulting from falls (Fig. 6 left) have been shown to fade (sublime) with time. Fanara et al. (2020b) have determined a minimum erosion rate of $\sim$0.3 m^3 per Mars year per metre along the scarp corresponding to a minimum average scarp retreat rate of $\sim$0.2 m/kyr. Both the NPLD and the BU scarps are active source areas of ice block falls (Su et al. 2023). The orbit characteristics and resolution make HiRISE the only imager capable of producing images for detailed analysis of these processes.

5.2 Swiss Cheese Features and Polar Layer Erosion

The south polar residual cap (SPRC) of Mars hosts a variety of features including quasi-circular depressions known as “Swiss cheese”. It is apparent from HiRISE observations that these depressions are increasing in size with time and that this rate is latitude dependent (e.g. Knightly et al. 2019; Cleveland et al. 2023). Variable haloes have been found around the depressions (Becerra and Byrne 2012) which may be related to the seasonally driven erosion process. Exposure of sub-surface water ice deposits may drive atmospheric water vapour production during southern summer (Innanen et al. 2022). These types of feature appear to be at too high latitude to be observed with CaSSIS and the evolution is too slow to be detectable with HRSC.

On the other hand, there is evidence of erosion of other layered structures at high southern latitudes (Fig. 7). The example in the figure shows bluish material on the scarp of a layer with more bluish material on the upper level suggesting wind-driven erosion (unlike the gully-like erosion seen in Sisyphi Cavi discussed below). Because of CO_2 ice coverage in winter, this must also be a seasonal effect.

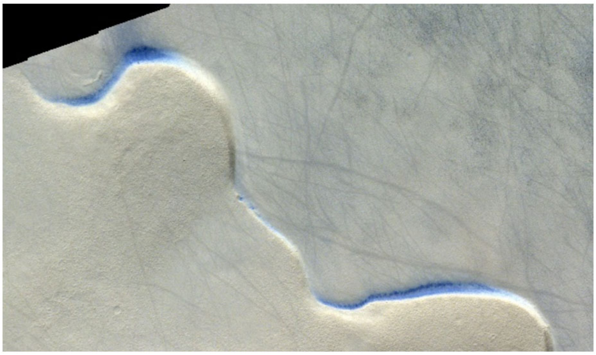

Fig. 7 Layered terrain east of Sisyphi Planum (9.8E, 72.2S). Blue coloured material is usually associated with mobile dust in CaSSIS images. Here (MY35_013935_280_0) bluish material can be seen on and close to the scarp which forms the dividing line between two terrain types. Credit: ESA/TGO/CaSSIS CC BY-SA 3.0 IGO

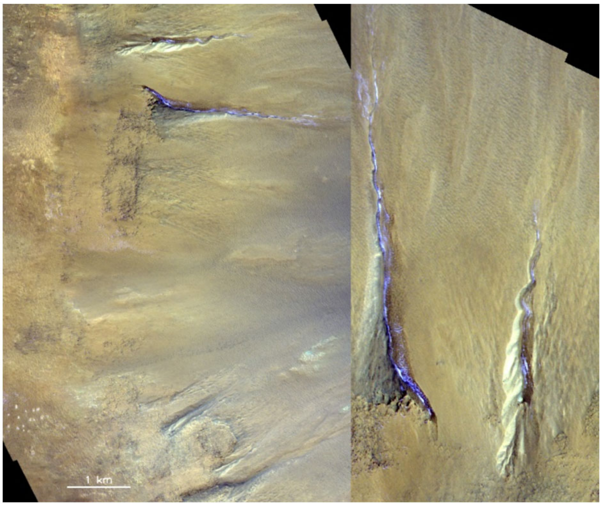

Fig. 8 CaSSIS image MY35_011076_242 (Coord 257.5E, 57.3S) showing gullies in Aonia Terra. The image was acquired at 11:35:30 local time at Ls=202.8. Left: Extract from georectified image. North is up. The two gullies to the top show the presence of ice. There are other small icy patches elsewhere to be seen. The gullies at the bottom appear to be older (more degraded) and frost/icy free at this time. Right: The gullies with ice have been extracted from the image, rotated (north is left) and expanded to enhance visibility of the ice within the gully structures. Credit: ESA/TGO/CaSSIS CC BY-SA 3.0 IGO

6 Ice-Related Seasonally Changes at Lower Latitudes

6.1 Ices in Gullies

Young gullies on Mars were first reported by Malin and Edgett (2000) and were initially suggested as evidence of recent liquid water flows on Mars (see also Mellon and Phillips 2001). Numerous formation mechanisms have subsequently been proposed (see Pasquon et al. 2019 and Khuller et al. 2021b for summaries). Since their discovery, monitoring of gullies (e.g. Pasquon et al. 2019) has revealed that they are active today at times of year when the Martian surface is at its coldest and when CO_2 ice is condensed on to the surface (Conway et al. 2020) – i.e. they are seasonally controlled. Formation through CO_2 related processes has been modelled by, for example, Pilorget and Forget (2016). CaSSIS imaging reveals the presence of persistent ice in gullies from winter through to late spring. The example in Fig. 8 shows ice or frost in the gullies at the top of the image. The image was acquired at 11:35:50 local solar time with the Sun at an incidence angle of 48.4° at an L_s of 202.8°. The bright material in the gullies is clearly visible, a higher resolution view (rotated) is provided on the left. Note that the gullies to the bottom of the right-hand image appear old,

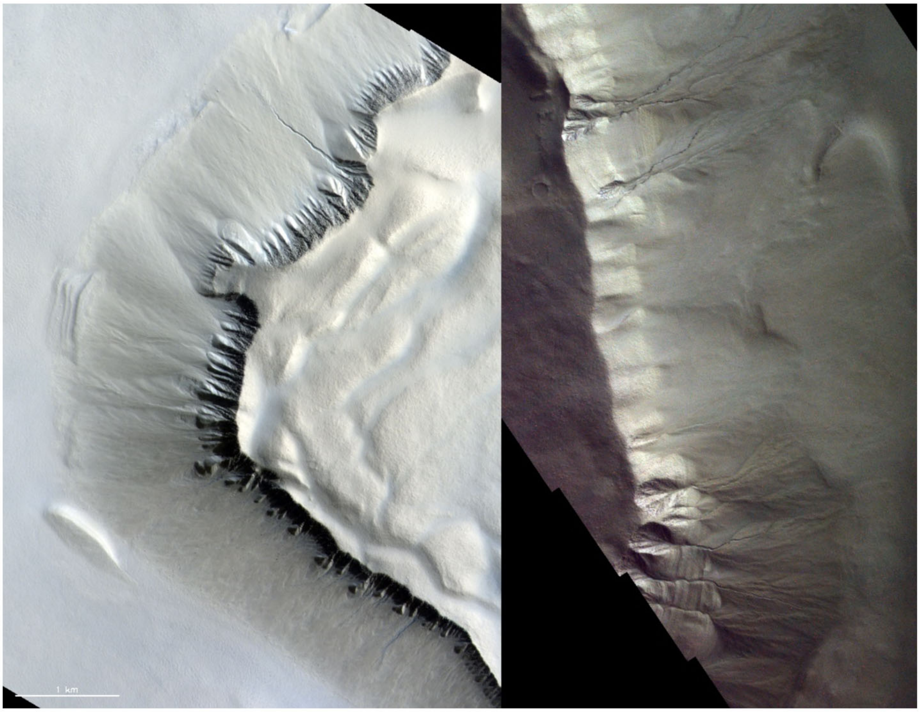

Fig. 9 CaSSIS images from the Sisyphi Cavi region showing recent gully activity Left: MY34_004583_256_0 (long./lat. 1.38°E, 71.2°S) acquired on 9 December 2018. Note the colluvial deposits (centre left) and the sinuous gully towards the top of the frame. Right: MY36_018111_253_0 (long./lat. 1.29°E, 68.4°S) acquired on 14 December 2021. Note here the more complex gully structure and the stratification (bottom centre). Credit: ESA/TGO/CaSSIS CC BY-SA 3.0 IGO

degraded, and do not show obvious signs of high reflectance material within them probably because of the lower variation in topographic relief and therefore more limited shadowing.

Dundas et al. (2022) have catalogued 300 recent flows in gullies using HiRISE data. The observations of sediment transport and the gully activity rates are consistent with gully formation entirely by CO_2 frost processes. No role for liquid water is required to explain the observations. Khuller and Christensen (2021a), however, suggest that in some areas, dusty water ice is present in the substrate and could melt (seasonally) to promote gully formation. Whereas liquid water is unlikely to explain current gully activity on Mars, melting of ice at the gully locations may have been possible at a higher tilt of the rotational axis, when partial melting of the ice caps raised the atmospheric pressure (Dickson et al. 2023).

Higher latitude gullies (e.g. Fig. 9) are also currently active (Raack et al. 2015). Seasonal modifications of a classical gully on a slope in Sisyphi Cavi (355E,71.5S) have been identified and there is an extensive dataset available for more thorough searches for such activity both at this site and elsewhere.

6.2 Frost Deposition

The Mars Orbiter Camera (MOC) and the Thermal Emission Spectrometer (TES) were employed to conduct the first studies of low latitude ice-related phenomena, revealing seasonal frost as low as 24°S on poleward-facing slopes (Schorghofer and Edgett 2006). Subsequent observations, conducted by the OMEGA and CRISM spectrometers, showed that seasonal water frost can be found on shadowed slopes at latitudes as low as 15°S and 32°N (Carrozzo et al. 2009; Vincendon et al. 2010). Even at equatorial latitudes of approximately 2°S, extremely small amounts of H_2O frost were observed to condense on the calibration targets of the Opportunity rover (Landis 2007).

TES 2 AM (local time) surface temperatures and thermal modeling were used by Cushing and Titus (2008) to demonstrate that CO_2 frost should form on the Arsia Mons caldera (∼9°S) every night of the year. Similarly, Piqueux et al. (2016), utilizing 3 AM measurements of atmospherically-corrected surface temperature from the Mars Climate Sounder (MCS) and thermal modelling, suggested that CO_2 frost condensation occurs on most equatorial, low thermal inertia regions at night and may persist up to an hour after sunrise. Lange et al. (2022) searched for these early morning frost deposits using Thermal Emission Imaging System (THEMIS) early morning data in equatorial, dusty regions but did not find evidence for early morning CO_2 frost.

Recent observations conducted using CaSSIS and HRSC indicate that frost condenses on the Tharsis volcanoes (Valantinas et al. 2024). The appearance clearly has a seasonal dependence but the detections were obtained during early morning indicating that a diurnal component may be also need to be accounted for. The Mars Global Climate Model (GCM) and the Weather Research and Forecasting (WRF) model suggest that the temperatures at the time of CaSSIS acquisitions are too warm for CO_2 frost to condense. Thus, the observed morning frost may be composed of H_2O. A tentative simultaneous detection by CaSSIS and the NOMAD spectrometer on TGO has been reported (Valantinas et al. 2024). Similar observations in the future may help better constrain the Martian volatile cycle.

Attempts to detect possible surface frost accumulations in the summit region of Olympus Mons continue. When imaging conditions allow, colour images of the caldera complex and surroundings are acquired from higher spacecraft altitudes at a range of local times, with a focus on morning images. Potential surface frost is most conspicuous in the blue channel of HRSC (440 ± 45 nm; Jaumann et al. 2007) and was tentatively observed in some images which were taken in very late northern winter (L_s ∼346° to 360°) at local times around 7 am, with incidence angles between 71° and 77° (Fig. 10a-c). The most reliable, but not definitive, evidence for frost comes from the differences in apparent surface brightness of the caldera floors, which do not seem to be caused by clouds. The most obvious changes in surface brightness are illustrated in Fig. 10c, where the floor of the north-easternmost caldera is distinctly brighter than, e.g., the southeastern part of the main (=oldest) caldera. This could be explained by the topography of the northeastern caldera which is the topographically deepest depression in the area (elevation difference is ∼1000 m from the floor to shoulder) and would act as the most efficient cold trap. In comparison, no evidence for possible surface frost is visible in other images with similar local times, more widely varying incidence angles and earlier in the season (L_s 328° to 346°) (Fig. 10d-f). However, the appearance of frost in images may be controlled by a variety of factors (e.g. surface thermal inertia, localised sub-surface cold trapping, etc.), and a full analysis of the influence of specific surface properties is presented in Valantinas et al. (2024).

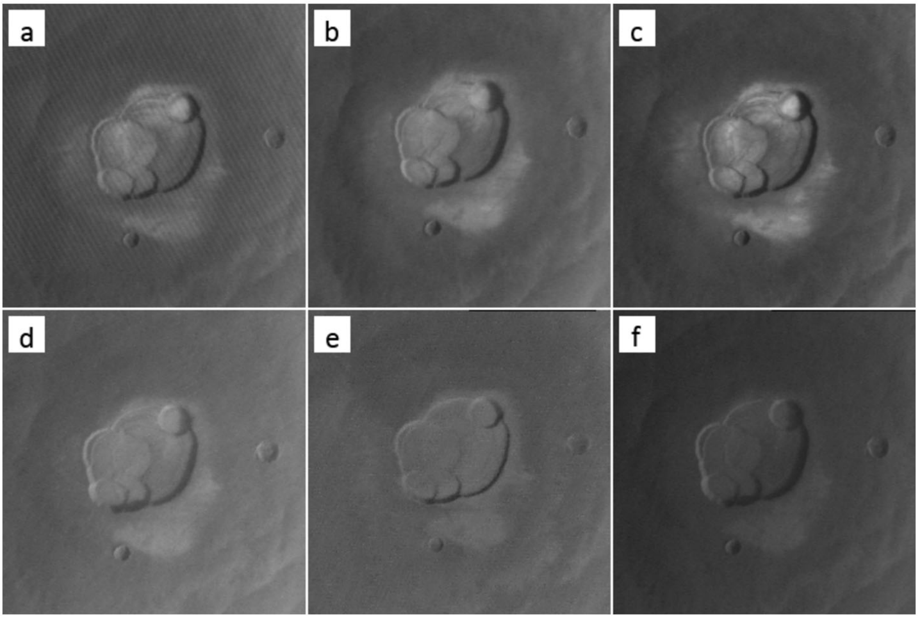

Fig. 10 Comparison of selected high-altitude HRSC blue channel (440 ± 45 nm) images of the Olympus Mons caldera region (North is up in all images, E-W diameter of caldera complex is about 73 km). Potential frost is visible as albedo difference inside the caldera complex in panels a-c, whereas the caldera surface appears uniform (no albedo differences) in panels d-f. (a) HRSC image hn889_0000; Ls 346.7°, local time 07:25 am, incidence angle 71.6°, imaging altitude 10,420 km, acquisition date 11 Nov 2022. (b) hn948_0000; Ls 355.7°, 07:01 am, 75.9°, 10,479 km, 17 Dec 2022. (c) hn963_0000; Ls 357.8°, 07:13 am, 72.8°, 9,633 km, 22 Dec 2022. (d) hn768_0000; Ls 328.0°, 07:14 am, 76.9°, 10,472 km, 26 Oct 2022. (e) hn772_0000; Ls 328.6°, 09:27 am, 48.8°, 9,401 km, 27 Oct 2022. (f) hn836_0000; Ls 338.6°, 06:57 am, 79.2°, 10,487 km, 15 Nov 2022. Credit: ESA/DLR/FU Berlin, CC BY-SA 3.0 IGO

7 Interaction with the Atmosphere

7.1 Observations of Recurring Slope Lineae (RSL)

Recurring Slope Lineae (RSL) are linear seasonal dark geomorphological features that are found on steep slopes in the equatorial and mid latitude regions (McEwen et al. 2011, 2014). RSLs are 100’s m long for few metres in width. The majority of them seem to originate from rocky terrains and they incrementally grow downhill. Their thickness is likely less than 10 cm because HiRISE images show no relief. The main distinguishing feature of RSLs is that they grow, fade and reform each year and appear when the soil reaches its maximum temperature (McEwen et al. 2011, 2014). RSLs have also been observed with CaSSIS (Fig. 11).

RSLs appear on steep slopes at equatorial and mid-latitudes with orientations that depend on the season. Liquid water related processes were initially proposed as an explanation for the RSLs (McEwen et al. 2011) effectively by process of elimination. Darkening of Martian simulants through wetting had previously been demonstrated by, for example, Gunderson et al. (2007). Deliquescence of salts (Ojha et al. 2014) was also suggested. Spectroscopic detection of hydrated salts using CRISM has been reported (Ojha et al. 2015) but more careful investigations demonstrated that this detection is not robust to noise (Vincendon et al.

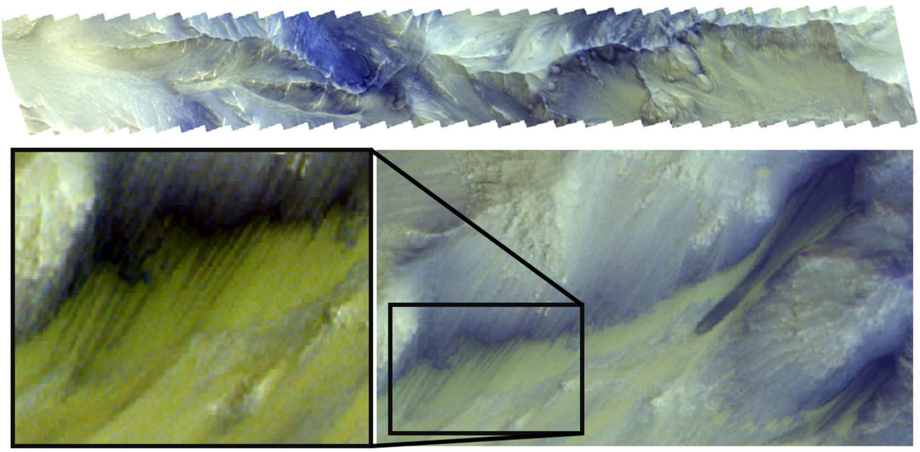

Fig. 11 CaSSIS image MY35_014188_345_0 shows RSL in Coprates Chasma. The expanded parts of the image below show the characteristic long thin structures appearing to run downslope. Credit: ESA/TGO/CaSSIS CC BY-SA 3.0 IGO

2019). In addition, an external atmospheric source of water is inconsistent with the atmospheric water vapour cycle (Stillman et al. 2016). On the other hand, an internal source of liquid water is also unlikely because many RSL are in isolated locations, such as near crater rims (Chojnacki et al. 2016) requiring a potentially unrealistic localization of near-surface water ice. Furthermore, thermal calculations constrained by THEMIS data show no evidence of liquid water (Edwards and Piqueux 2016). The final termination of the RSL was identified to be related to the angle of repose of dry sand suggesting granular flow with limited inertia (Schmidt et al. 2017; Dundas et al. 2017). Local thermal calculations (Millot et al. 2021) and precise photometry and colour analysis using HiRISE and CaSSIS data (Munaretto et al. 2021, 2022) appear to confirm a dry process with no activity at diurnal timescales (Munaretto et al. 2020). Analysis of data after the Planet-Encircling Dust Event (PEDE) of 2018 (McEwen et al. 2021) suggest that RSL formation and growth are strongly favored during the aftermath of dust storms. Dust may directly cause RSL formation (Schaefer et al. 2019; Vincendon et al. 2019), or dust storms may correlate with some other factor, such as sand transport, that facilitates RSL activity.

An alternative concept of wet processes with seasonality has been proposed. When the sun illuminates granular soil in rarefied atmospheric conditions such as Mars, it has been demonstrated experimentally that the soil could act as a Knudsen pump (de Beule et al. 2013). This model has been adapted for granular material (Schmidt et al. 2017) to explain RSL seasonality in a fully dry process. The angle of repose, modified by the air flux within the pores of the sand, is seasonal but not enough to trigger a flow. In the shadow of a boulder, an enhanced Knudsen pump could occur, triggering the flow with the correct seasonal/orientation pattern in agreement with the observation (Schmidt et al. 2017). An experimental validation of these forces has been conducted (Bila et al. 2023).

Finally, aeolian mechanisms have been proposed to explain the origin and formation of RSL. Vincendon et al. (2019) proposes formation of the incrementally lengthening dark streaks by dust removal by winds, locally enhanced by topographic reliefs (i.e., venturi-like effects). Dundas (2020) proposes that RSL are formed by aeolian grainflows that displace surficial dust, thereby creating dark streaks. The modelling by Stillman et al. (2021) finds partial correlations between sediment transport regimes and RSL activity, tentatively explaining RSL as the results of transported sediments (i.e., grains) during high aeolian activity periods.

7.2 Seasonally-Related Surface Hydration

OMEGA/MEx has provided evidence for mineral hydration of the entire Martian surface in the form of a ubiquitous absorption band at 3 μm in the infrared (Jouglet et al. 2007). This strong and broad band is caused by fundamental vibrations of the -OH hydroxyl group and the H_2O molecule and the exact form of hydration, its mineral carriers and its variability are still the topic of active research. The amount of OH/H_2O present in the surface layer is estimated (model-dependent) to be in the range of a few wt. % with regional and latitudinal variations (Milliken et al. 2007). Water adsorption in equilibrium with atmospheric vapor and responding to diurnal and seasonal cycles had initially been thought to be a main contributor to this signature. However, the stability of the band throughout the season over most of the surface and the general absence of a 1.9 μm band as well as comparisons with behaviors observed when simulating adsorption processes with Martian dust analogues in the lab (Pommerol et al. 2009; Beck et al. 2010) do not support this hypothesis. Instead, this strong feature is probably caused by more strongly bound water/hydroxyls produced during aqueous weathering of rocks in the Noachian and continuously released and mixed into the surface dust by slow mechanical erosion of the ancient crust (Audouard et al. 2014; Beck et al. 2015). Some spectral variability observed at higher latitude (>50°) is however consistent with active exchange between surface, subsurface and atmosphere. Poulet et al. (2008) observe changes in the strengths of both the 1.9 and 3 μm band that indicate variations of hydration in response to changes in atmospheric vapor content and/or diffusive exchange with ice deeper below the surface. Both processes could be important aspects of the water cycle at seasonal and longer timescales but the amount of water involved and the exchange kinetics remain largely unconstrained. Recent re-analysis of the OMEGA dataset has also revealed previously unseen spectral variability in the shape of the 3 μm band over a ring at high northern latitudes (Stcherbinine et al. 2021). No change with time of the year or time of the day has been observed and the presently favored hypothesis involves the presence of stable hydrated salts, probably sulphates or perchlorates.

8 Imaging of Seasonal Dust Activity

8.1 Larger Scale Dust Events

Seasonal changes in the observed dust activity on Mars (i.e. large-scale dust storms) have been known for many decades (e.g. Kahn et al. 1992) and lead to significant surface changes (Geissler 2005; Geissler et al. 2016). Planet-encircling dust events (PEDEs) are seen on average less than once per decade (Cantor and Malin 2018) and occur during southern summer. The most recent instances have been in 2007 and 2018 (e.g. Zurek et al. 2018). The largest non-global events are also seen during this period. Although near-global in extent, MEx/VMC observations have shown that while dust penetrated into the polar cap region in 2018 it never covered the cap completely. The spatial distribution was both inhomogeneous and rapidly changing (Hernández-Bernal et al. 2019). Global climate models predict changes in dust coverage before and after global storms (Bapst et al. 2022) and indeed vast areas of Mars show annual variations in surface albedo both associated with dust storms and in their absence - depending on location and season (Wellington and Bell 2020). In

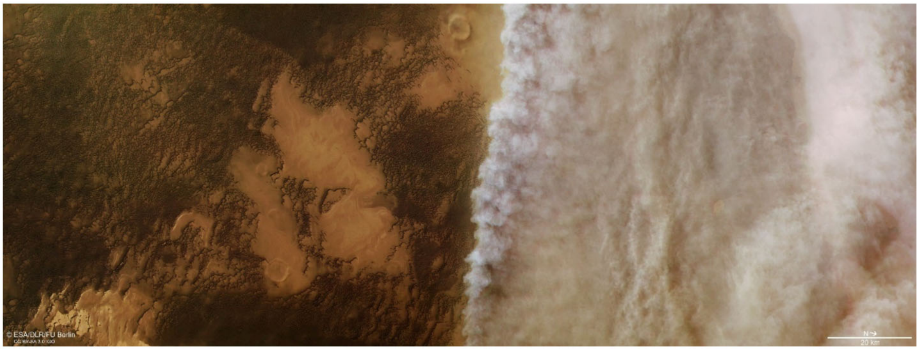

Fig. 12 HRSC observation hi039_0000 of a local dust storm front north of Utopia Planitia. North is to the right and the image width (left to right) covers around 200 km of the Martian surface. Credit: ESA/DLR/FU Berlin, CC BY-SA 3.0 IGO

contrast to the relatively quiescent deposition of dust over broad areas associated with seasonal decreases in atmospheric opacity, storms can provide an important reset to regions that experience significant dust removal (Wellington and Bell 2020) through episodic transport, erosion, and deposition of sediment (Chojnacki 2018). Evidence of larger events is present both in the MARCI and HRSC data sets. Figure 12 is one of the nicest examples from HRSC and shows an ∼90 km wide front with extensive atmospheric dust content to the right of the front.

8.2 Local Weather Observed Through Remote Sensing

As on Earth, local weather is also a seasonal phenomenon on Mars and smaller, local, atmosphere-surface interaction via aeolian processes that have a seasonally-controlled component can occur. Observations of Martian clouds have been made using orbital remote sensing since the Viking era (e.g. Kahn 1984) and clouds are evident in the HRSC, CaSSIS, VMC, and MARCI data sets (e.g. Fernando et al. 2023). While high altitude clouds are of scientific interest, in tis work we are interested in tropospheric dust clouds as indicators of movement of surface materials. CaSSIS has seen evidence of dust transport probably arising from aeolian processes in combination with atmospheric pressure gradients (Fig. 13). The field of view is not sufficient to identify the full extent of activity in most observed cases but combination with global monitoring imagers (e.g. MARCI) is certainly feasible although not fully exploited at this time.

It should also be noted that CaSSIS took occasional images during the PEDE of 2018 to assess opacity. The highest optical depth images show structure in the dust distribution on sub-km length scales which might indicate something about the mixing in the troposphere but there have been no efforts to date to exploit this information.

9 Short-Term Dust-Related Surface Phenomena

Slope streaks (Fig. 14) are a type of active morphological feature found on dusty Martian slopes that gradually fade over decadal timescales (Bergonio et al. 2013; Morris 1982; Schorghofer et al. 2007). Unlike RSL, which exhibit high seasonality, slope streak formation appears to be weakly correlated with season (Heyer et al. 2019). Furthermore, slope streaks

Fig. 13 CaSSIS image MY35_011368_288 showing a possible weather front in Aonia Terra. The black scale bar to the left is 1 km long. Credit: ESA/TGO/CaSSIS CC BY-SA 3.0 IGO

tend to occur on shallower slopes than RSL, with terminal segments of slope streaks having a median value of 16 degrees (below the angle of repose) (Brusnikin et al. 2016), while RSL exhibit terminal slope angles of approximately 30 degrees (Dundas et al. 2017). Prior to the discovery of RSL, there was a debate regarding the formation mechanism of slope streaks, ranging from aqueous to dry in origin (Ferguson and Lucchitta 1984; Kreslavsky and Head 2009; Schorghofer et al. 2002; Williams 1991). However, subsequent spectroscopic studies did not reveal hydration bands that could indicate the presence of water (Amador et al. 2016). Geomorphological analysis also supports the concept that dark slope streaks form as ground-hugging, low-density avalanches of dry surface dust (Dundas 2020).

One of the most notable characteristics of slope streaks is their variable photometric properties (Fig. 14). Although most slope streaks are darker than their surroundings by up to 10% (Sullivan et al. 2001), there is a considerable population of bright slope streaks in Arabia Terra that are up to 4% brighter than their surroundings (Valantinas et al. 2021). The bright streaks have been identified as older dark slope streaks (Schorghofer et al. 2007; Valantinas et al. 2021). It has been suggested that the brightening mechanism might be related to either dust deposition (Aharonson et al. 2003) or the degradation of surface agglomerates leading to surface compaction (Valantinas et al. 2021).

Dust devil tracks, on the other hand, are typically found on flat terrains and form via dust deflation by moving dust devils. Dust devils are atmospheric vortices and they are made visible to remote sensing instruments by the dust being lifted by pressure gradients and associated winds. Their spatial and temporal distribution, shape, and velocity provide insight into local atmospheric dynamics, and can be useful for, for example, weather and climate modelling (Reiss et al. 2014, 2016). Local observations near landing sites have also been presented (e.g. Jackson 2022). They are often easily visible from Mars orbit appearing to be bright and considerably less red than the surface itself. The frequency distribution is seasonally dependent (e.g. Stanzel et al. 2008; Fenton and Lorenz 2015). This is an almost ideal application for machine learning algorithms (Fig. 16). Conway et al. (2022) and Bickel et al. (2023) have scanned the CaSSIS data set and made a preliminary statistical analysis showing the seasonal and local time distributions of identified dust devils. Most of the available orbital image datasets have not been thoroughly scanned for dust devils and/or are limited to images acquired at a fixed local time (sun-synchronous orbits), limiting the representativeness of current analyses. The results expand upon previous observations. The maximum of dust devil activity at midday through to early afternoon is also evident in observations from Curiosity (Jackson 2022).

The appearance and vanishing of dust devil tracks also have a seasonal component as dust devils preferentially occur at certain seasons, depending on the geographic region on Mars

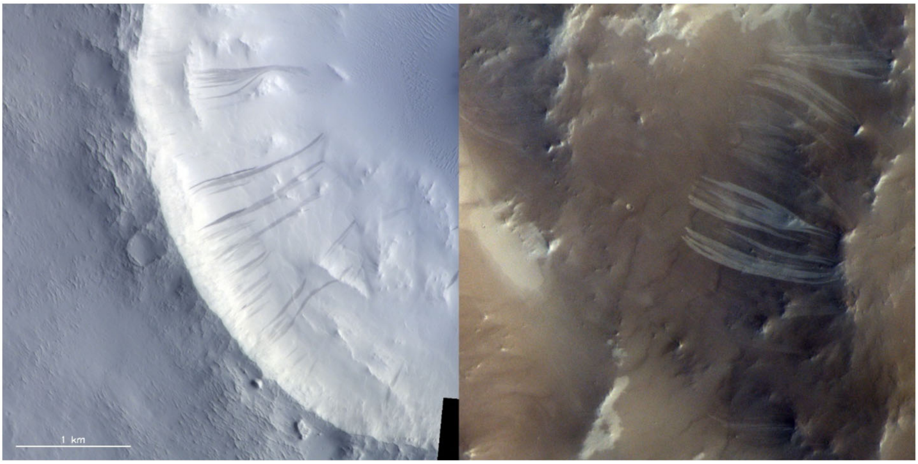

Fig. 14 Dark and bright slope streaks in Arabia Terra acquired by CaSSIS. Left: Dark slope streaks (long.,lat. 28.89°E, 25.94°N) acquired on 5 July 2021 (MY36_015964_025_0). Right: Bright slope streaks (long.,lat. 33.97°E, 20.87°N) seen at low phase angle (11.7°) on 10 May 2023 (MY37_024386_022_3). Credit: ESA/TGO/CaSSIS CC BY-SA 3.0 IGO

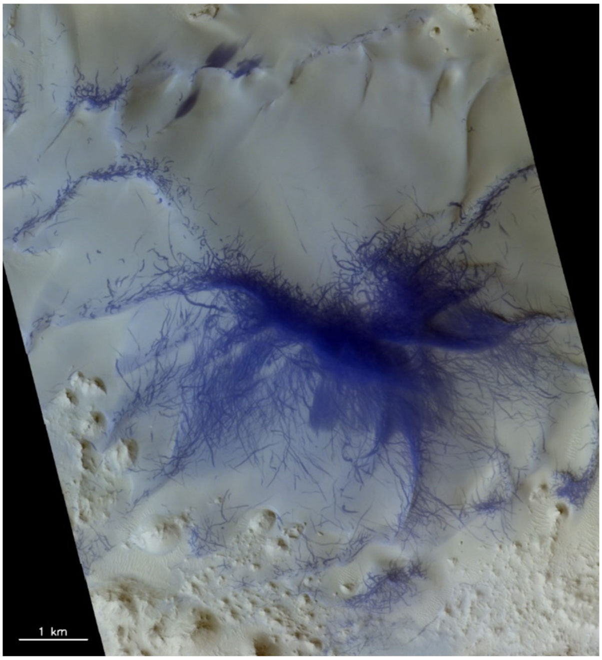

Fig. 15 Image of dust devil tracks. Longitude 57.1°E, latitude 25.9°N. North is up. This image is a composite NIR-PAN-BLU image from CaSSIS (MY34_005400_153_1). The strong blue colour usually indicates dusty, dune-forming, material in these CaSSIS products. Note the concentration of dust devil tracks on the ridges in this area. Credit: ESA/TGO/CaSSIS CC BY-SA 3.0 IGO

(Cantor et al. 2006; Reiss et al. 2011, 2016). The resulting dark tracks (Fig. 15) usually fade within a Martian season (Malin and Edgett 2001; Balme et al. 2003). Some dust devil tracks have been shown to disappear completely after global dust storms (Greeley et al. 2010). It has been suggested that dust devil tracks can be eliminated by the deposition of merely a few microns of airfall dust (Malin and Edgett 2001; Wells et al. 1984). Dust devil tracks are only

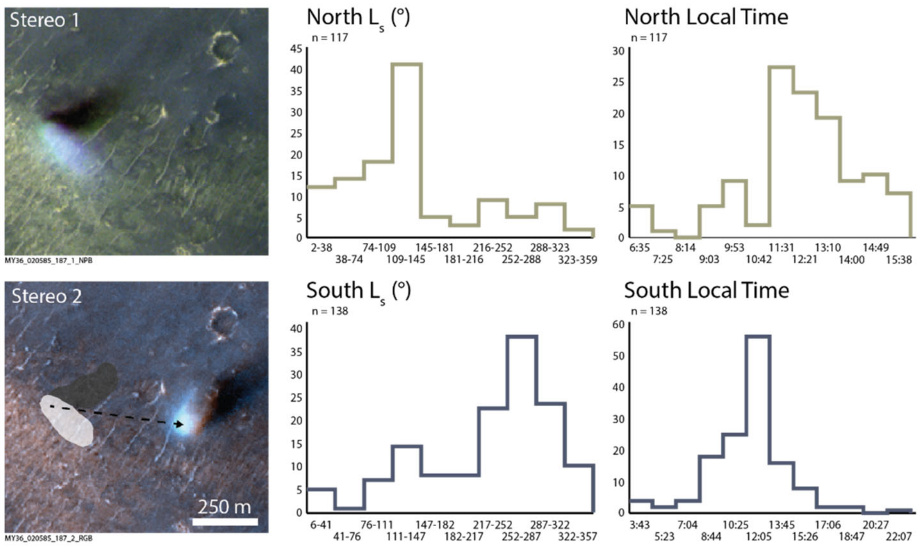

Fig. 16 Left: A stereo observation taken by CaSSIS of a dust devil. The apparent motion can be measured through the time delay between the two observations (roughly 45 seconds). Centre: Frequency distributions of CaSSIS observations of dust devils against Ls (Martian season) for the northern hemisphere (top) and the southern hemisphere (bottom). Right: Frequency distributions of CaSSIS observations of dust devils against local time for the northern hemisphere (top) and the southern hemisphere (bottom). Credit: ESA/TGO/CaSSIS CC BY-SA 3.0 IGO

approximately 5% darker than their surroundings (Munaretto et al. 2022), which indicates that the surface may be less rough than that of slope streaks. Interestingly, some dust devil tracks may also appear brighter than the substrate in which they form (Reiss et al. 2011). In laboratory experiments, it has been observed that the passage of dust devils can induce re-orientation of individual dust grains, leading to a more densely packed and reflective surface (Pendleton Hoffer and Greeley 2010). It should be noted that different preparation methods produce photometric differences in granular simulants. Another proposed mechanism for the formation of bright dust devil tracks involves the smoothing of the dust aggregate layer, which results in a slight increase in albedo (Reiss et al. 2011).

Since dust devils do not stop their travel at dune fields, changes of dust devil tracks are a further type of seasonal modification of the appearance of dunes. Whereas dust devil tracks on floors of dune-exhibiting craters have been reported in several studies (e.g., Fenton et al. 2005; Sullivan et al. 2008; Verba et al. 2010) only few studies exist about dust devil tracks on dune bodies themselves (e.g., Verba et al. 2010; Bennett et al. 2017). One reason might be that dust devil tracks preferably develop on slow-moving and immobile dunes (Bennett et al. 2017) because the (dune) surface in question must be covered with dust that is erased/lifted away by the dust devil leaving the typically low-albedo streaks behind (Reiss et al. 2013, 2016). Bennett et al. (2017) found dust devil streaks on the dunes in Syrtis Major in almost every of their studied CTX images between MY 29 and 32. Although dust fallout by dust storms is not a seasonal process, it is worth noting here that dust devil tracks on dunes are more evident and frequent after dust storm events, because the settling dust after the storm increases the albedo of the dune (and thus the contrast to the tracks, Bennett et al. (2017)) and provides the dust layer needed by dust devils to leave behind the tracks.

10 Ripple and Dune Migration

The migration of entire dune bodies, but particularly the migration of small to meter-scale ripples, is also subject to a seasonal component (e.g. Chojnacki et al. 2022), because migration occurs preferentially in windy seasons and during major storm events. There is a wealth of studies on this topic, most of them are based on analyses of high-resolution HiRISE data. Since this process is less the focus of the seasonal changes discussed here, we refer the interested reader to the large body of published literature (e.g., Bourke et al. 2008; Sullivan et al. 2008; Silvestro et al. 2010; Hansen et al. 2011; Silvestro et al. 2011, 2013; Ayoub et al. 2014; Chojnacki et al. 2014; Baker et al. 2018; Silvestro et al. 2020; Chojnacki et al. 2021) with the comprehensive review of activities on modern Mars by Diniega et al. (2021) particularly recommended.

11 Landing Sites and Impact Changes

Evidence for hyper-velocity impacts onto the surface of Mars by small meteorites was first presented by Malin et al. (2006). A catalogue of recent impacts has been presented by Daubar et al. (2022). The blast zones arising and the exposure of sub-surface ices (Byrne et al. 2009) are visible from orbit but are transient with the surface broadly returning photometrically to its previous state after some time. Daubar et al. (2016) have quantified this and concluded that the average lifetime among sites with measurable fading is $\sim$15 Mars years. The fading is probably not linear and they note that at approximately half the sites with three or more repeat images with HiRISE, a nonlinear function with rapid initial fading followed by a slow increase in albedo provides a better fit to the fading behaviour (Daubar et al. 2016).

Although CaSSIS has an inferior spatial resolution, these effects can also be monitored as indicated in Fig. 17 which shows an impact site formed between August 2020 and February 2021 in an image acquired by CaSSIS on 9 July 2023. The vicinity of the impact is strongly blue in CaSSIS colour products possibly as a result of dust on the surface or the exposure of a compositionally different substrate.

12 Concluding Remarks

The combination of very high resolution with intermediate resolution colour filtered data acquired at different local times has provided new insights into the seasonally-driven phenomena occurring on Mars today. Many of the observations have required sub-decametre resolution, precise targeting (both spatially and temporally), and high photometric performance. Coverage remains an issue because there are many more sites that warrant monitoring than can be imaged at the required frequency. This is especially true of the dynamic phenomena associated with the sublimation of the seasonal caps. Limitations to the scientific return resulting from a low (<75°) inclination orbit are also present in the TGO dataset. Nonetheless, progress has been made in assessing and understanding many of the observables and it is evident that the scientific aims of future instruments can be better focused as a result of the multi-spacecraft activities to date.

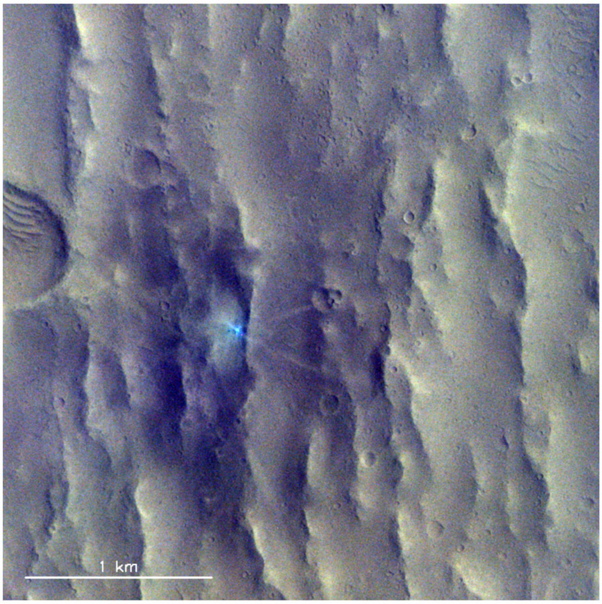

Fig. 17 Impact site in Sacra Sulci acquired by CaSSIS on 9 July 2023 (MY37_025092_162_0). The impact was formed between August 2020 and February 2021. Blue colours are usually associated with dust. Strong reflections from ice in the blue are also possible sources for the observed colour but this would imply a lifetime for surficial water ice that far exceeds that expected from modelling. In this case, the effect of the substrate composition may be significant. See also HiRISE image ESP_077597_1980. Credit: ESA/TGO/CaSSIS CC BY-SA 3.0 IGO

13 Open Questions

We provide here a list of open questions which arise from the observations of seasonal processes made to date. Some of these questions are related to similar ideas expressed in Smith et al. (2020) which focussed on polar science.

1. Do small and mid-scale seasonal processes alter the climate record preserved in polar layered deposits and, if so, how?

2. How does global and regional dust activity influence seasonal volatile cycles? Does this influence reach circum-polar areas? To what extent do seasonal cap properties vary with/without global dust storms?

3. Does the regolith play a significant role in the water cycle through adsorption/diffusion processes?

4. Why is there a "cryptic region" and why only in the south?

5. Why has no growth of large araneiforms yet been detected? Are they geologically relative old (as our crude calculations would suggest)?

6. How do regolith and substrate properties influence seasonal processes?

7. Are polar scarps in equilibrium between ablation and flow?

8. Is the near-surface polar weather accurately described by current General Circulation Models?

9. What hazards might seasonal processes present to the manned exploration of Mars? Alternatively, what advantages might they bring?

10. It can be seen that H_2O plays a role in the evolution of the seasonal caps. But are the processes really understood?

11. Despite considerable effort, the processes driving RSL and their seasonal behaviour remain elusive. What exactly is the process?

12. Is salt deliquescence a widespread and significant process?

13. Do low-latitude diurnal frosts influence surface evolution?

It is apparent that progress on most of the questions can only be made through further data acquisition. On the other hand, the questions are diverse and will probably require a variety of approaches to data collection through, for example, orbital remote sensing, landed atmospheric networks, and mobile surface analysis.

Perhaps the largest advances at this stage could be achieved through a mobile landed system operating within the polar region(s). The word "rover" is associated with a wheeled device but the use of aerial platforms (e.g. "helicopters") to inspect polar-layered terrains or exposed water-ice scarps (for example) and increase accessibility has already been proposed (e.g. Bapst et al. 2021; Smith et al. 2022). One key point of note is that contact with icy surfaces drains heat from any landed element driving power and thermal design issues. If a concept to alleviate these issues can be established (clearly some form of nuclear power must be considered) then long-lived mobile polar-based platforms (with appropriate instrumentation) could make considerable in-roads into our open question list. Measurement of atmospheric composition, atmospheric dust content and opacity, condensation rates, surface pressures and wind characteristics over a full Martian year at high latitude would provide considerable constraints on atmospheric transport processes for example.

Acknowledgements The authors would like to thank the editors for their support and our colleagues on the HRSC and CaSSIS teams. The authors wish to thank the spacecraft and instrument engineering teams for the successful completion of the instrument. CaSSIS is a project of the University of Bern and funded through the Swiss Space Office via ESA's PRODEX programme. The instrument hardware development was also supported by the Italian Space Agency (ASI) (ASI-INAF agreement no.I/018/12/0), INAF/Astronomical Observatory of Padova, and the Space Research Center (CBK) in Warsaw. Support from SGF (Budapest), the University of Arizona (Lunar and Planetary Lab.) and NASA are also gratefully acknowledged. Operations support from the UK Space Agency under grant ST/R003025/1 is also acknowledged.

Funding Open access funding provided by University of Bern.

Declarations

Competing Interests The authors are active members of the European Mars community and receive financing to maintain the data acquisition of the CaSSIS and HRSC instruments. No funding was received to assist with the preparation of this manuscript.

References

Acharya P, Smith IB, Calvin W (2024) Tracking the south polar seasonal cap retreat of Mars using computer vision. Icarus 417:116104. https://doi.org/10.1016/j.icarus.2024.116104

Aharonson O, Schorghofer N, Gerstell MF (2003) Slope streak formation and dust deposition rates on Mars. J Geophys Res, Planets 108(E12). https://doi.org/10.1029/2003JE002123

Aharonson O, Zuber MT, Smith DE, Neumann GA, Feldman WC, Prettyman TH (2004) Depth, distribution, and density of CO_2 deposition on Mars. J Geophys Res 109(E5):E05004. https://doi.org/10.1029/2003JE002223

Alsaeed NR, Hayne PO (2022) Transport of water into the polar regions of Mars through scavenging by CO_2 snowfall. J Geophys Res, Planets 127:e2022JE007386. https://doi.org/10.1029/2022JE007386

Amador ES, Mushkin A, Gillespie A (2016) Spectral characteristics of dark slope streaks on Mars: a global survey with CRISM. In: 47th Annual Lunar and Planetary Science Conference, p 2696

Appéré T, Schmitt B, Langevin Y, Douté S, Pommerol A, Forget F, Spiga A, Gondet B, Bibring J-P (2011) Winter and spring evolution of northern seasonal deposits on Mars from OMEGA on Mars Express. J Geophys Res, Planets 116:E05001

Audouard J, Poulet F, Vincendon M, Milliken RE, Jouglet D, Bibring J-P, Gondet B, Langevin Y (2014) Water in the Martian regolith from OMEGA/Mars Express. J Geophys Res, Planets 1969. https://doi.org/10.1002/2014JE004649oi

Aye K-M, Schwamb ME, Portyankina G, Hansen CJ, McMaster A, Miller GRM, Carstensen B, Snyder C, Parrish M, Lynn S, Mai C, Miller D, Simpson RJ, Smith AM (2019) Planet four: probing springtime winds on Mars by mapping the southern polar CO_2 jet deposits. Icarus 319:558. https://doi.org/10.1016/j.icarus.2018.08.018

Ayoub F, Avouac JP, Newman CE, Richardson MI, Lucas A, Leprince S, Bridges NT (2014) Threshold for sand mobility on Mars calibrated from seasonal variations of sand flux. Nat Commun 5:5096. https://doi.org/10.1038/ncomms6096

Baker MM, Lapotre MGA, Minitti ME, Newman CE, Sullivan R, Weitz CM, Rubin DM, Vasavada AR, Bridges NT, Lewis KW (2018) The bagnold dunes in southern summer: active sediment transport on Mars observed by the Curiosity rover. Geophys Res Lett 45:8853–8863. https://doi.org/10.1029/2018GL079040

Balme MR, Whelley PL, Greeley R (2003) Mars: Dust devil track survey in Argyre Planitia and Hellas Basin. J Geophys Res, Planets 108(E8). https://doi.org/10.1029/2003JE002096

Bapst J, Parker TJ, Balaram J, Tzanetos T, Matthies LH, Edwards CD, Freeman A, Withrow-Maser S, Johnson W, Amador-French E, Bishop JL, Daubar IJ, Dundas CM, Fraeman AA, Hamilton CW, Hardgrove C, Horgan B, Leung CW, Lin Y, Mittelholz A, Weiss BP (2021) Mars science helicopter: compelling science enabled by an aerial platform. Bull Am Astron Soc 53:361. https://doi.org/10.3847/25c2cfeb.a126aea0

Bapst J, Piqueux S, Edwards CS, Wolfe C, Hayne PO, Kass DM, Kleinböhl A (2022) Surface dust redistribution on Mars from interannual differences in temperature and albedo. J Geophys Res, Planets 127:e2022JE007365. https://doi.org/10.1029/2022JE007365

Becerra P, Byrne S (HiRISE Team) (2012) CO_2 frost halos on the south polar residual cap of Mars. In: 43rd Annual Lunar and Planetary Science Conference, p 2513

Beck P, Pommerol A, Schmitt B, Brissaud O (2010) Kinetics of water adsorption on minerals and the breathing of the Martian regolith. J Geophys Res, Planets E10011. https://doi.org/10.1029/2009JE003539oi

Beck P, Pommerol A, Zanda B, Remusat L, Lorand JP, Göpel C, Hewins R, Pont S, Lewin E, Quirico E, Schmitt B, Montes-Hernandez G, Garenne A, Bonal L, Proux O, Hazemann JL, Chevrier VF (2015) A Noachian source region for the “Black Beauty” meteorite, and a source lithology for Mars surface hydrated dust? Earth Planet Sci Lett 104. https://doi.org/10.1016/j.epsl.2015.06.033oi

Bennett KA, Fenton L, Bell JF (2017) The albedo of Martian dunes: insights into aeolian activity and dust devil formation. Aeolian Res 26:89–100. https://doi.org/10.1016/j.aeolia.2016.08.009

Bergonio JR, Rottas KM, Schorghofer N (2013) Properties of Martian slope streak populations. Icarus 225(1):194–199. https://doi.org/10.1016/j.icarus.2013.03.023

Bibring J-P, Langevin Y, Poulet F, Gendrin A, Gondet B, Berthé M, Soufflot A, Drossart P, Combes M, Bellucci G, Moroz V, Mangold N, Schmitt B, OMEGA Team Erard, Erard S, Forni O, Manaud N, Poulleau G, Encrenaz T, Fouchet T, Melchiorri R, Altieri F, Formisano V, Bonello G, Fonti S, Capaccioni F, Cerroni P, Coradini A, Kottsov V, Ignatiev N, Titov D, Zasova L, Pinet P, Sotin C, Hauber E, Hoffman H, Jaumann R, Keller U, Arvidson R, Mustard J, Duxbury T, Forget F (2004b) Perennial water ice identified in the south polar cap of Mars. Nature 428:627.

Bibring J-P, Soufflot A, Berthé M, Langevin Y, Gondet B, Drossart P, Bouyé M, Combes M, Puget P, Semery A, Bellucci G, Formisano V, Moroz V, Kottsov V, Bonello G, Erard S, Forni O, Gendrin A, Manaud N, Poulet F, Poulleau G, Encrenaz T, Fouchet T, Melchiori R, Altieri F, Ignatiev N, Titov D, Zasova L, Coradini A, Capacionni F, Cerroni P, Fonti S, Mangold N, Pinet P, Schmitt B, Sotin C, Hauber E, Hoffmann H, Jaumann R, Keller U, Arvidson R, Mustard J, Forget F (2004a) OMEGA: observatoire pour la Minéralogie, l'Eau, les Glaces et l'Activité. In: Wilson A (ed) Mars Express: the scientific payload. ESA SP-1240, 37

Bickel VT, Conway SJ, Thomas N, Read M, Valantinas A, Hauber E, Grindrod P, Wray J, Rangarajan V, CaSSIS Science Team (2023) Exploring CaSSIS with machine learning - the search for dust devils on Mars. LPI contributions, vol 2806, p 1479

Bila T, Kollmer J, Teiser J, Wurm G (2023) Thermal creep on Mars: visualizing a soil layer under tension. Planet Sci J, Am Astron Soc 4:16. https://doi.org/10.3847/psj/acaaaa

Bourke M, Edgett KS, Cantor BA (2008) Recent eolian dune change on Mars. Geomorphology 94:247–255

Brusnikin ES, Kreslavsky MA, Zubarev AE, Patratiy VD, Krasilnikov SS, Head JW, Karachevtseva IP (2016) Topographic measurements of slope streaks on Mars. Icarus 278:52–61. https://doi.org/10.1016/j.icarus.2016.06.005
Byrne S (2009) The polar deposits of Mars. Annu Rev Earth Planet Sci 37:535. https://doi.org/10.1146/annurev.earth.031208.100101
Byrne S Murray BC (2002) North polar stratigraphy and the paleo-erg of Mars. J Geophys Res Planets 107:5044. https://doi.org/10.1029/2001JE001615
Byrne S, Dundas CM, Kennedy MR, Mellon MT, McEwen AS, Cull SC, Daubar IJ, Shean DE, Seelos KD, Murchie SL, Cantor BA, Arvidson RE, Edgett KS, Reufer A, Thomas N, Harrison TN, Posiolova LV, Seelos FP (2009) Distribution of mid-latitude ground ice on Mars from new impact craters. Science 325:1674. https://doi.org/10.1126/science.1175307
Calvin WM, James PB, Cantor BA, Dixon EM (2015) Interannual and seasonal changes in the North polar ice deposits of Mars: observations from MY 29-31 using MARCI. Icarus 251:181. https://doi.org/10.1016/j.icarus.2014.08.026
Calvin WM, Cantor BA, James PB (2017) Interannual and seasonal changes in the south seasonal polar cap of Mars: observations from MY 28-31 using MARCI. Icarus 292:144. https://doi.org/10.1016/j.icarus.2017.01.010
Cantor BA, Malin MC (2018) MRO MARCI observations of the evolution of the 2018 planet-encircling dust event. AGU Fall Meet Abstr 2018:P34A-01
Cantor BA, Kanak KM, Edgett KS (2006) Mars Orbiter Camera observations of Martian dust devils and their tracks (September 1997 to January 2006) and evaluation of theoretical vortex models. J Geophys Res, Planets 111. https://doi.org/10.1029/2006JE002700
Carrozzo FG, Bellucci G, Altieri F, D'Aversa E, Bibring J-P (2009) Mapping of water frost and ice at low latitudes on Mars. Icarus 203(2):406–420
Cesar C, Pommerol A, Thomas N, Portyankina G, Hansen CJ, Tornabene LL, Munaretto G, Cremonese G (2022) Seasonal southern circum-polar spots and araneiforms observed with the Colour and Stereo Surface Imaging System (CaSSIS). Planet Space Sci 224:105593. https://doi.org/10.1016/j.pss.2022.105593
Chevrier VF, Fitting AB, Rivera-Valentín EG (2022) Limited stability of multicomponent brines on the surface of Mars. Planet Sci J 3:125. https://doi.org/10.3847/PSJ/ac6603
Chicarro A, Martin P, Trautner R (2004) The Mars Express mission: an overview. In: Wilson A (ed) Mars Express: the scientific payload. ESA SP-1240, 3
Chojnacki M (2018) Aeolian surface transport in response to the 2018 planet-encircling dust storm. AGU Fall Meet Abstr 2018:P43J–3861
Chojnacki M, Johnson JR, Moersch JE, Fenton LK, Michaels TI, Bell JF (2014) Persistent aeolian activity at endeavour crater, meridiani planum, Mars; new observations from orbit and the surface. Icarus. https://doi.org/10.1016/j.icarus.2014.04.044
Chojnacki M, McEwen A, Dundas C, Ojha L, Urso A, Sutton S (2016) Geologic context of recurring slope lineae in Melas and Coprates Chasmata. Mars J Geophys Res Planets 121:1204–1231. https://doi.org/10.1002/2015je004991
Chojnacki M, Vaz DA, Silvestro S, Silva DCA (2021) Widespread megaripple activity across the North polar ergs of Mars. J Geophys Res, Planets 126:e2021JE006970. https://doi.org/10.1029/2021JE006970
Chojnacki M, Vaz DA, Silvestro S, Silva DCA (2022) Annual variability of dune field fluxes on Mars. In: 53rd Lunar and Planetary Science Conference, 2678, p 2064
Cleveland RD, Chevrier V, Tullis JA (2023) Object-based image analysis of "Swiss cheese" pitted terrains' evolution on the Martian south polar cap. In: 54th Lunar and Planetary Science Conference, 2806, p 2726.
Conway S, Pommerol A, Raack J, Philippe M, McEwen A, Thomas N, Cremonese G (2020) Gullies on Mars and seasonal ices visualised using the Colour and Stereo Surface Imaging System (CaSSIS), EGU General Assembly 2020, Online, 4–8 May 2020, EGU2020-21643. https://doi.org/10.5194/egusphere-egu2020-21643
Conway SJ, Bickel VT, Patel MR, Fenton L, Carson H (2022) Global survey of dust devils in CTX data using neural networks. In: 53rd Lunar and Planetary Science Conference, 2678, p 1874.
Cushing GE, Titus TN (2008) MGS-TES thermal inertia study of the Arsia Mons Caldera. J Geophys Res, Planets 113(E6)
Daubar IJ, Dundas CM, Byrne S, Geissler P, Bart GD, McEwen AS, Russell PS, Chojnacki M, Golombek MP (2016) Changes in blast zone albedo patterns around new Martian impact craters. Icarus 267:86. https://doi.org/10.1016/j.icarus.2015.11.032
Daubar IJ, Dundas CM, McEwen AS, Gao A, Wexler D, Piqueux S, Collins GS, Miljkovic K, Neidhart T, Eschenfelder J, Bart GD, Wagstaff KL, Doran G, Posiolova L, Malin M, Speth G, Susko D, Werynski A (2022) New craters on Mars: an updated catalog. J Geophys Res, Planets 127:e07145. https://doi.org/10.1029/2021JE007145

de Beule C, Wurm G, Kelling T, Kupper M, Jankowski T, Teiser J (2013) The Martian soil as a planetary gas pump. Nat Phys 10:17–20. https://doi.org/10.1038/nphys2821

de Villiers S, Nermoen A, Jamtveit B, Mathiesen J, Meakin P, Werner SC (2012) Formation of Martian araneiforms by gas-driven erosion of granular material. Geophys Res Lett 39. https://doi.org/10.1029/2012GL052226

Dickson JL, et al (2023) Gullies on Mars could have formed by melting of water ice during periods of high obliquity. Science 380:1363–1367. https://doi.org/10.1126/science.abk2464

Diniega S, Byrne S, Bridges NT, Dundas CM, McEwen AS (2010) Seasonality of present-day Martian dune-gully activity. Geology 38:1047–1050. https://doi.org/10.1130/G31287.1

Diniega S, Hansen CJ, Allen A, Grigsby N, Li Z, Perez T, Chojnacki M (2019) Dune-slope activity due to frost and wind throughout the North polar erg. Mars Geol Soc London Spec Publ 467:95–114. https://doi.org/10.1144/sp467.6

Diniega S, Bramson AM, Buratti B, Buhler P, Burr DM, Chojnacki M, Conway SJ, Dundas CM, Hansen CJ, McEwen AS, Lapôtre MGA, Levy J, Mc Keown L, Piqueux S, Portyankina G, Swann C, Titus TN, Widmer JM (2021) Modern Mars' geomorphological activity, driven by wind, frost, and gravity. Geomorphology 380:107627. https://doi.org/10.1016/j.geomorph.2021.107627

Dinwiddie CL, Titus TN (2021) Airborne dust plumes lofted by dislodged ice blocks at Russell crater, Mars. Geophys Res Lett 48:e91920. https://doi.org/10.1029/2020gl091920

Douté S, Schmitt B, Langevin Y, Bibring J-P, Altieri F, Bellucci G, Gondet B, Poulet F, Mex OMEGA Team (2007) South pole of Mars: nature and composition of the icy terrains from Mars Express OMEGA observations. Planet Space Sci 55:113. https://doi.org/10.1016/j.pss.2006.05.035

Douté S, Wu C, Guo X, Luo B (2015) Defrosting processes on the Russell crater megadune of Mars: quantitative analysis and interpretation. EPSC2015-2533

Dundas CM (2020) An aeolian grainflow model for Martian recurring slope lineae. Icarus 343:113681

Dundas CM, McEwen AS, Chojnacki M, Milazzo MP, Byrne S, McElwaine JN, Urso A (2017) Granular flows at recurring slope lineae on Mars indicate a limited role for liquid water. Nat Geosci 10(12):903–907. https://doi.org/10.1038/s41561-017-0012-5

Dundas CM, Conway SJ, Cushing GE (2022) Martian gully activity and the gully sediment transport system. Icarus 386:115133. https://doi.org/10.1016/j.icarus.2022.115133

Edwards CS, Piqueux S (2016) The water content of recurring slope lineae on Mars. Geophys Res Lett 43:8912–8919. https://doi.org/10.1002/2016gl070179

Fanara L, Gwinner K, Hauber E, Oberst J (2020a) Present-day erosion rate of North polar scarps on Mars due to active mass wasting. Icarus 342:113434. https://doi.org/10.1016/j.icarus.2019.113434

Fanara L, Gwinner K, Hauber E, Oberst J (2020b) Automated detection of block falls in the North polar region of Mars. Planet Space Sci 180:104733. https://doi.org/10.1016/j.pss.2019.104733

Fedorova AA, Rodin AV, Baklanova IV (2004) Seasonal cycle of water vapor in the atmosphere of Mars as revealed from the MAWD/Viking 1 and 2 experiment. Sol Syst Res 38:421. https://doi.org/10.1007/s11208-005-0009-2

Fenton LK, Lorenz R (2015) Dust devil height and spacing with relation to the Martian planetary boundary layer thickness. Icarus 260:246. https://doi.org/10.1016/j.icarus.2015.07.028

Fenton LK, Toigo AD, Richardson MI (2005) Aeolian Processes in Proctor Crater on Mars: Mesoscale modeling of dune-forming winds. J Geophys Res 110. https://doi.org/10.1029/2004JE002309

Ferguson HM, Lucchitta BK (1984) Dark streaks on talus slopes. Mars: 188–190

Fernando AM, Wolff MJ, Forget F (2023) Seasonal variations of orographic clouds on Mars with MRO/MARCI observations and the Mars planetary climate model. Icarus 400:115559. https://doi.org/10.1016/j.icarus.2023.115559

Gardin E, Allemand P, Quantin C, Thollot P (2010) Defrosting, dark flow features, and dune activity on Mars: Example in Russell crater. J Geophys Res, Planets 115. https://doi.org/10.1029/2009JE003515

Gary-Bicas CE, Hayne PO, Horvath T, Heavens NG, Kass DM, Kleinböhl A, Piqueux S, Shirley JH, Schofield JT, McCleese DJ (2020) Asymmetries in snowfall, emissivity, and albedo of Mars' seasonal polar caps: Mars Climate Sounder observations. J Geophys Res, Planets 125:e06150. https://doi.org/10.1029/2019JE006150

Geissler PE (2005) Three decades of Martian surface changes. J Geophys Res, Planets 110:E02001. https://doi.org/10.1029/2004JE002345

Geissler PE, Fenton LK, Enga M-T, Mukherjee P (2016) Orbital monitoring of Martian surface changes. Icarus 278:279. https://doi.org/10.1016/j.icarus.2016.05.023

Giuranna M, Hansen G, Formisano V, Zasova L, Maturilli A, Grassi D, Ignatiev N (2007) Spatial variability, composition and thickness of the seasonal North polar cap of Mars in mid-spring. Planet Space Sci 55:1328. https://doi.org/10.1016/j.pss.2007.03.006

Giuranna M, Grassi D, Formisano V, Montabone L, Forget F, Zasova L (2008) PFS/MEX observations of the condensing CO_2 south polar cap of Mars. Icarus 197:386. https://doi.org/10.1016/j.icarus.2008.05.019

Greeley R, Waller DA, Cabrol NA, Landis GA, Lemmon MT, Neakrase LDV, et al (2010) Gusev Crater, Mars: Observations of three dust devil seasons. J Geophys Res, Planets 115(E7). https://doi.org/10.1029/2010JE003608

Gunderson K, Lüthi B, Russell P, Thomas N (2007) Visible/NIR photometric signatures of liquid water in Martian regolith simulant. Planet Space Sci 55:1272. https://doi.org/10.1016/j.pss.2007.03.004

Gwinner K, Jaumann R, Hauber E, Hoffmann H, Heipke C, Oberst J, Neukum G, Ansan V, Bostelmann J, Dumke A, Elgner S, Erkeling G, Fueten F, Hiesinger H, Hoekzema NM, Kersten E, Loizeau D, Matz K-D, McGuire PC, Mertens V, Michael G, Pasewaldt A, Pinet P, Preusker F, Reiss D, Roatsch T, Schmidt R, Scholten F, Spiegel M, Stesky R, Tirsch D, van Gasselt S, Walter S, Wählisch M, Willner K (2016) The High Resolution Stereo Camera (HRSC) of Mars Express and its approach to science analysis and mapping for Mars and its satellites. Planet Space Sci 126:93–138. https://doi.org/10.1016/j.pss.2016.02.014

Haberle RM, Kahre MA (2010) Detecting secular climate change on Mars. Int J Mars Sci Explor 4:68. https://doi.org/10.1555/mars.2010.0003

Hansen GB (1997) The infrared absorption spectrum of carbon dioxide ice from 1.8 to 333 μm. J Geophys Res 102:21569. https://doi.org/10.1029/97JE01875

Hansen GB (2013) An examination of Mars' North seasonal polar cap using MGS: composition and infrared radiation balance. Icarus 225:869. https://doi.org/10.1016/j.icarus.2013.02.019

Hansen CJ, Thomas N, Portyankina G, McEwen A, Becker T, Byrne S, Herkenhoff K, Kieffer H, Mellon M (2010) HiRISE observations of gas sublimation-driven activity in Mars' southern polar regions: I. Erosion of the surface. Icarus, MRO/HiRISE Stud Mars 205:283–295. https://doi.org/10.1016/j.icarus.2009.07.021

Hansen CJ, Bourke M, Bridges NT, Byrne S, Colon C, Diniega S, Dundas C, Herkenhoff K, McEwen A, Mellon M, Portyankina G, Thomas N (2011) Seasonal erosion and restoration of Mars' northern polar dunes. Science 331:575

Hansen CJ, Byrne S, Portyankina G, Bourke M, Dundas C, McEwen A, Mellon M, Pommerol A, Thomas N (2013) Observations of the northern seasonal polar cap on Mars: I. Spring sublimation activity and processes. Icarus 225:881. https://doi.org/10.1016/j.icarus.2012.09.024

Hansen C, Conway S, Portyankina G, Thomas N, McEwen A, Perry J, Pommerol A, Cesar C (2019) Searching for seasonal jets on Mars in CaSSIS and HiRISE images. EPSC-DPS2019-388

Hansen CJ, Conway S, Portyankina G, Thomas N, McEwen AS (2020) Searching for seasonal jets on Mars in CaSSIS and HiRISE images. In: 51st Annual Lunar and Planetary Science Conference, p 2351

Hao J, Michael GG, Adeli S, Jaumann R (2019) Araneiform terrain formation in Angustus Labyrinthus, Mars. Icarus 317:479–490. https://doi.org/10.1016/j.icarus.2018.07.026

Herkenhoff KE, Byrne S, Russell PS, Fishbaugh KE, McEwen AS (2007) Meter-scale morphology of the North polar region of Mars. Science 317:1711. https://doi.org/10.1126/science.1143544

Hernández-Bernal J, Sánchez-Lavega A, del Río-Gaztelurrutia T, Hueso R, Cardesín-Moinelo A, Ravanis EM, de Burgos-Sierra A, Titov D, Wood S (2019) The 2018 Martian Global Dust Storm over the south polar region studied with MEx/VMC. Geophys Res Lett 46:10330. https://doi.org/10.1029/2019GL084266

Hess SL, Ryan JA, Tillman JE, Henry RM, Leovy CB (1980) The annual cycle of pressure on Mars measured by Viking Landers 1 and 2. Geophys Res Lett 7:197. https://doi.org/10.1029/GL007i003p00197

Heyer T, Kreslavsky M, Hiesinger H, Reiss D, Bernhardt H, Jaumann R (2019) Seasonal formation rates of Martian slope streaks. Icarus 323:76. https://doi.org/10.1016/j.icarus.2019.01.010

Horgan BHN, Bell JF III (2012) Seasonally active slipface avalanches in the North polar sand sea of Mars: evidence for a wind-related origin. Geophys Res Lett 39:L09201. https://doi.org/10.1029/2012gl051329

Horváth A, Kereszturi A, Bérczi S, Sik A, Pócs T, Gánti T, Szathmáry E (2009) Analysis of dark albedo features on a southern polar dune field of Mars. Astrobiology 9:90–103. https://doi.org/10.1089/ast.2007.0212

Huebner WF, Benkhoff J, Capria M-T, Coradini A, De Sanctis C, Orosei R, Prialnik D (2006) Heat and Gas Diffusion in Comet Nuclei. ISSI Scientific Report, SR-004

Innanen AC, Landis ME, Hayne PO, Moores JE (2022) Possible atmospheric water vapor contribution from Martian Swiss cheese terrain. Planet Sci J 3:242. https://doi.org/10.3847/PSJ/ac979e

Jackson B (2022) Vortices and dust devils as observed by the Mars environmental dynamics analyzer instruments on board the Mars 2020 perseverance rover. Planet Sci J 3:20. https://doi.org/10.3847/PSJ/ac4586

James PB, Kieffer HH, Paige DA (1992) The seasonal cycle of carbon dioxide on Mars. In: Kieffer HH, Jakosky BM, Snyder CW, Matthews MS (eds) Mars (A93-27852 09-91). Univ. Arizona Press, p 934

Jaumann R, Neukum G, Behnke T, Duxbury TC, Eichentopf K, Flohrer J, et al (2007) The high-resolution stereo camera (HRSC) experiment on Mars Express: instrument aspects and experiment conduct from interplanetary cruise through the nominal mission. Planet Space Sci 55(7):928–952. https://doi.org/10.1016/j.pss.2006.12.003

Jouannic G, Gargani J, Costard F, Ori GG, Marmo C, Schmidt F, Lucas A (2012) Morphological and mechanical characterization of gullies in a periglacial environment: the case of the Russell crater dune (Mars). Planet Space Sci 71:38–54. https://doi.org/10.1016/j.pss.2012.07.005

Jouglet D, Poulet F, Milliken RE, Mustard JF, Bibring J-P, Langevin Y, Gondet B, Gomez C (2007) Hydration state of the Martian surface as seen by Mars Express OMEGA: 1. Analysis of the 3 μm hydration feature. J Geophys Res, Planets: E08S06. https://doi.org/10.1029/2006JE002846oi

Kahn R (1984) The spatial and seasonal distribution of Martian clouds and some meteorological implications. J Geophys Res 89:6671. https://doi.org/10.1029/JA089iA08p06671

Kahn RA, Martin TZ, Zurek RW, Lee SW (1992) The Martian dust cycle. In: Kieffer HH, Jakosky BM, Snyder CW, Matthews MS (eds) Mars (A93-27852 09-91). Univ. Arizona Press, p 1017

Kelly NJ, Boynton WV, Kerry K, Hamara D, Janes D, Reedy RC, Kim KJ, Haberle RM (2006) Seasonal polar carbon dioxide frost on Mars: CO_2 mass and columnar thickness distribution. J Geophys Res, Planets 111:E03S07. https://doi.org/10.1029/2006JE002678

Kereszturi A, Möhlmann D, Bérczi S, Ganti T, Horvath A, Kuti A, Pocs T, Szathmary E (2008) Analysis of possible interfacial water driven seepages on Mars. In: 39th Annual Lunar and Planetary Science Conference, p 1555

Kereszturi A, Horvath A, Sik A, Kuti A, Bérczi S, Gánti T, Pócs T, Szathmáry E (2009a) Possible liquid-like water produced seepage features on Mars. In: 40th Annual Lunar and Planetary Science Conference, p 1111

Kereszturi A, Möhlmann D, Berczi S, Ganti T, Kuti A, Sik A, Horvath A (2009b) Recent rheologic processes on dark polar dunes of Mars: driven by interfacial water? Icarus 201:492–503

Kereszturi A, Möhlmann D, Berczi S, Ganti T, Horvath A, Kuti A, Sik A, Szathmary E (2010) Indications of brine related local seepage phenomena on the northern hemisphere of Mars. Icarus 207:149–164

Khayat ASJ, McConnochie TH, Smith MD (2022) The annual cycle of water vapor above Gale crater as retrieved by CRISM and compared to ChemCam passive sky spectroscopy. Icarus 385:115136. https://doi.org/10.1016/j.icarus.2022.115136

Khuller AR, Christensen PR (2021a) Evidence of exposed dusty water ice within Martian gullies. J Geophys Res, Planets 126:e2020JE006539. https://doi.org/10.1029/2020JE006539

Khuller AR, Christensen PR, Harrison TN, Diniega S (2021b) The distribution of frosts on Mars: links to present day gully activity. J Geophys Res, Planets 126:e06577. https://doi.org/10.1029/2020JE006577

Kieffer HH (2000) Annual punctuated CO_2 slab-ice and jets on Mars. In: Second international conference on Mars polar science and exploration, p 93

Kieffer HH (2007) Cold jets in the Martian polar caps. J Geophys Res, Planets 112. https://doi.org/10.1029/2006JE002816

Kieffer HH, Titus TN, Mullins KF, Christensen PR (2000) Mars south polar spring and summer behavior observed by TES: seasonal cap evolution controlled by frost grain size. J Geophys Res, Planets 105:9653–9699. https://doi.org/10.1029/1999JE001136

Kieffer HH, Christensen PR, Titus TN (2006) CO_2 jets formed by sublimation beneath translucent slab ice in Mars' seasonal south polar ice cap. Nature 442:793–796. https://doi.org/10.1038/nature04945

Kirk RL, Brown RH, Soderblom LA (1990) Subsurface energy storage and transport for solar-powered geysers on Triton. Science 250:424. https://doi.org/10.1126/science.250.4979.424

Kirk RL, Fergason RL, Redding B, Galuszka D, Smith E, Mayer D, Hare TM, Gwinner K (2020) Evaluating stereo DTM quality at jezero crater, Mars with HRSC, Ctx, and hirise images, ISPRS. Int Arch Photogramm Remote Sens Spat Inf Sci 43B3:1129. https://doi.org/10.5194/isprs-archives-XLIII-B3-2020-1129-2020

Kirk RL, Mayer D, Redding BL, Galuszka DM, Fergason RL, Hare TM, Gwinner K (2021) Further adventures in Mars DTM quality: smoothing errors, sharpening details, ISPRS - international archives of the photogrammetry. Remote Sens Spat Inf Sci 43B3:659. https://doi.org/10.5194/isprs-archives-XLIII-B3-2021-659-2021

Knightly JP, Fusco MS, Farnsworth K, Chevrier VF (2019) Temporal variations of Swiss cheese terrain. In: 50th Annual Lunar and Planetary Science Conference, p 2187

Kreslavsky MA, Head JW (2009) Slope streaks on Mars: a new "wet" mechanism. Icarus 201(2):517–527. https://doi.org/10.1016/j.icarus.2009.01.026

Kuzmin RO, Zabalueva EV, Evdokimova NA, Christensen PR (2012) Mapping of the water ice content within the Martian surficial soil on the periphery of the retreating seasonal northern polar cap based on the TES and the OMEGA data. J Geophys Res, Planets 117:E00J19. https://doi.org/10.1029/2012JE004071

Landis GA (2007) Observation of frost at the equator of Mars by the opportunity rover. In: 38th Annual Lunar and Planetary Science Conference, abstract 2433. Retrieved from http://adsabs.harvard.edu/abs/2007LPI....38.2423L

Lange L, Piqueux S, Edwards CS (2022) Gardening of the Martian regolith by diurnal CO_2 frost and the formation of slope streaks. J Geophys Res, Planets 127(4):e2021JE006988

Langevin Y, Gondet B (2020) Observations of the polar caps of Mars by OMEGA/Mex in the visible range. In: Seventh international conference on Mars polar science and exploration, 2099, pp 6043
Langevin Y, Douté S, Vincendon M, Poulet F, Bibring J-P, Gondet B, Schmitt B, Forget F (2006) No signature of clear CO_2 ice from the 'cryptic' regions in Mars' south seasonal polar cap. Nature 442:790. https://doi.org/10.1038/nature05012
Langevin Y, Bibring J-P, Montmessin F, Forget F, Vincendon M, Douté S, Poulet F, Gondet B (2007) Observations of the south seasonal cap of Mars during recession in 2004-2006 by the OMEGA visible/near-infrared imaging spectrometer on board Mars Express. J Geophys Res, Planets 112:E08S12. https://doi.org/10.1029/2006JE002841
Laskar J, Levrard B, Mustard JF (2002) Orbital forcing of the Martian polar layered deposits. Nature 419:375. https://doi.org/10.1038/nature01066
Leighton RB, Murray BC (1966) Behavior of carbon dioxide and other volatiles on Mars. Science 153:136. https://doi.org/10.1126/science.153.3732.136
Määttänen A, Mathé C, Audouard J, Listowski C, Millour E, Forget F, González-Galindo F, Falletti L, Bardet D, Teinturier L, Vals M, Spiga A, Montmessin F (2022) Troposphere-to-mesosphere microphysics of carbon dioxide ice clouds in a Mars global climate model. Icarus 385:115098. https://doi.org/10.1016/j.icarus.2022.115098
Malin MC, Edgett KS (2000) Evidence for recent groundwater seepage and surface runoff on Mars. Science 288:2330. https://doi.org/10.1126/science.288.5475.2330
Malin MC, Edgett KS (2001) Mars Global Surveyor Mars Orbiter Camera: interplanetary cruise through primary mission. J Geophys Res, Planets 106(E10):23429–23570. https://doi.org/10.1029/2000JE001455
Malin MC, Edgett KS, Posiolova LV, McColley SM, Dobrea EZN (2006) Present-day impact cratering rate and contemporary gully activity on Mars. Science 314:1573. https://doi.org/10.1126/science.1135156
Malin MC, Bell JF, Cantor BA, Caplinger MA, Calvin WM, Clancy RT, Edgett KS, Edwards L, Haberle RM, James PB, Lee SW, Ravine MA, Thomas PC, Wolff MJ (2007) Context camera investigation on board the Mars reconnaissance orbiter. J Geophys Res, Planets 112:E05S04. https://doi.org/10.1029/2006JE002808
Maltagliati L, Titov DV, Encrenaz T, Melchiorri R, Forget F, Keller HU, Bibring J-P (2011) Annual survey of water vapor behavior from the OMEGA mapping spectrometer onboard Mars Express. Icarus 213:480. https://doi.org/10.1016/j.icarus.2011.03.030
Mangold N, Costard F, Forget F (2003) Debris flows over sand dunes on Mars: Evidence for liquid water. J Geophys Res, Planets 108. https://doi.org/10.1029/2002JE001958
McEwen AS, Eliason EM, Bergstrom JW, Bridges NT, Hansen CJ, Delamere WA, Grant JA, Gulick VC, Herkenhoff KE, Keszthelyi L, Kirk RL, Mellon MT, Squyres SW, Thomas N, Weitz CM (2007) Mars reconnaissance orbiter's high resolution imaging science experiment (HiRISE). J Geophys Res, Planets 112:E05S02. https://doi.org/10.1029/2005JE002605
McEwen AS, Ojha L, Dundas CM, Mattson SS, Byrne S, Wray JJ, Cull SC, Murchie SL, Thomas N, Gulick VC (2011) Seasonal flows on warm Martian slopes. Science 333:740–743. http://www.sciencemag.org/content/333/6043/740.abstract
McEwen AS, Dundas CM, Mattson SS, Toigo AD, Ojha L, Wray JJ, Chojnacki M, Byrne S, Murchie SL, Thomas N (2014) Recurring slope lineae in equatorial regions of Mars. Nat Geosci 7:53–58. https://doi.org/10.1038/ngeo2014
McEwen AS, Schaefer EI, Dundas CM, Sutton SS, Tamppari LK, Chojnacki M (2021) Mars: abundant Recurring Slope Lineae (RSL) Following the Planet Encircling Dust Event (PEDE) of 2018. J Geophys Res, Planets 126:e06575. https://doi.org/10.1029/2020JE006575
McKeown LE, Bourke MC, McElwaine JN (2017) Experiments on sublimating carbon dioxide ice and implications for contemporary surface processes on Mars. Sci Rep 7:14181. https://doi.org/10.1038/s41598-017-14132-2
McKeown L, McElwaine JN, Bourke MC, Sylvest ME, Patel MR (2021) The formation of araneiforms by carbon dioxide venting and vigorous sublimation dynamics under Martian atmospheric pressure. Sci Rep 11:6445. https://doi.org/10.1038/s41598-021-82763-7
Mellon MT, Phillips RJ (2001) Recent gullies on Mars and the source of liquid water. J Geophys Res 106:23165. https://doi.org/10.1029/2000JE001424
Milliken RE, Mustard JF, Poulet F, Jouglet D, Bibring J-P, Gondet B, Langevin Y (2007) Hydration state of the Martian surface as seen by Mars Express OMEGA: 2. H_2O content of the surface. J Geophys Res, Planets: E08S07. https://doi.org/10.1029/2006JE002853oi
Millot C, Quantin-Nataf C, Leyrat C, Enjolras M (2021) Local topography effects on the surface temperatures on Mars – application to the case of Recurring Slope Lineae (RSL). Icarus 355:114136. https://doi.org/10.1016/j.icarus.2020.114136
Morris EC (1982) Aureole deposits of the Martian volcano Olympus Mons. J Geophys Res, Solid Earth 87(B2):1164–1178. https://doi.org/10.1029/JB087iB02p01164

Munaretto G, Pajola M, Cremonese G, Re C, Lucchetti A, Simioni E, McEwen AS, Pommerol A, Becerra P, Conway SJ, Thomas N, Massironi M (2020) Implications for the origin and evolution of Martian recurring slope lineae at Hale crater from CaSSIS observations. Planet Space Sci 187:104947

Munaretto G, Pajola M, Lucchetti A, Re C, Cremonese G, Simioni E, Cambianica P, Thomas N (2021) Topographic correction of HiRISE and CaSSIS images: validation and application to color observations of Martian albedo features. Planet Space Sci 200:105198

Munaretto G, Pajola M, Lucchetti A, Cremonese G, Simioni E, Re C, et al (2022) Multiband photometry of Martian Recurring Slope Lineae (RSL) and dust-removed features at Horowitz crater, Mars from TGO/CaSSIS color observations. Planet Space Sci 214:105443. https://doi.org/10.1016/j.pss.2022.105443

Murchie S, Arvidson R, Bedini P, Beisser K, Bibring J-P, Bishop J, Boldt J, Cavender P, Choo T, Clancy RT, Darlington EH, Des Marais D, Espiritu R, Fort D, Green R, Guinness E, Hayes J, Hash C, Heffernan K, Hemmler J, Heyler G, Humm D, Hutcheson J, Izenberg N, Lee R, Lees J, Lohr D, Malaret E, Martin T, McGovern JA, McGuire P, Morris R, Mustard J, Pelkey S, Rhodes E, Robinson M, Roush T, Schaefer E, Seagrave G, Seelos F, Silverglate P, Slavney S, Smith M, Shyong W-J, Strohbehn K, Taylor H, Thompson P, Tossman B, Wirzburger M, Wolff M (2007) Compact Reconnaissance Imaging Spectrometer for Mars (CRISM) on Mars Reconnaissance Orbiter (MRO). J Geophys Res, Planets 112:E05S03. https://doi.org/10.1029/2006JE002682

Neukum G, Jaumann R (2004) HRSC: the High Resolution Stereo Camera of Mars Express, in Mars Express: the Scientific Payload, ESA-SP 1240, 17

Ojha L, McEwen A, Dundas C, Byrne S, Mattson S, Wray J, Masse M, Schaefer E (2014) HiRISE observations of Recurring Slope Lineae (RSL) during southern summer on Mars. Icarus 231:365–376. https://doi.org/10.1016/j.icarus.2013.12.021

Ojha L, Wilhelm MB, Murchie SL, McEwen AS, Wray JJ, Hanley J, Massé M, Chojnacki M (2015) Spectral evidence for hydrated salts in recurring slope lineae on Mars. Nat Geosci 8:829–832. https://doi.org/10.1038/ngeo2546

Oliva F, D'Aversa E, Bellucci G, Carrozzo FG, Ruiz Lozano L, Altieri F, Thomas IR, Karatekin O, Cruz Mermy G, Schmidt F, Robert S, Vandaele AC, Daerden F, Ristic B, Patel MR, López-Moreno J-J, Sindoni G (2022) Martian CO_2 ice observation at high spectral resolution with ExoMars/TGO NOMAD. J Geophys Res, Planets 127:e07083. https://doi.org/10.1029/2021JE007083

Ormston T, Denis M, Scuka D, Griebel H (2011) An ordinary camera in an extraordinary location: outreach with the Mars webcam. Acta Astronaut 69(7–8):703–713. https://doi.org/10.1016/j.actaastro.2011.04.015

Paige DA, Ingersoll AP (1985) Annual heat balance of Martian polar caps: Viking observations. Science 228:1160. https://doi.org/10.1126/science.228.4704.1160

Paige DA, Bachman JE, Keegan KD (1994) Thermal and albedo mapping of the polar regions of Mars using Viking thermal mapper observations 1. North polar region. J Geophys Res 99:25959. https://doi.org/10.1029/93JE03428

Pankine AA (2022) Martian atmospheric water vapor abundances in MY26-30 from Mars Express PFS/LW observations. Icarus 379:114975. https://doi.org/10.1016/j.icarus.2022.114975

Pasquon K, Gargani J, Massé M, Vincendon M, Conway SJ, Séjourné A, Jomelli V, Balme MR, Lopez S, Guimpier A (2019) Present-day development of gully-channel sinuosity by carbon dioxide gas supported flows on Mars. Icarus 329:296. https://doi.org/10.1016/j.icarus.2019.03.034

Pendleton Hoffer M, Greeley R (2010) Bright tracks on Mars: alternate dust devil tracks. In: 41st Annual Lunar and Planetary Science Conference, pp 2713. Retrieved from https://ui.adsabs.harvard.edu/abs/2010LPI....41.2713P

Pilorget C, Forget F (2016) Formation of gullies on Mars by debris flows triggered by CO_2 sublimation. Nat Geosci 9:65. https://doi.org/10.1038/ngeo2619

Piqueux S, Christensen PR (2008) North and south subice gas flow and venting of the seasonal caps of Mars: a major geomorphological agent. J Geophys Res, Planets 113:E06005. https://doi.org/10.1029/2007je003009

Piqueux S, Byrne S, Richardson MI (2003) Sublimation of Mars's southern seasonal CO_2 ice cap and the formation of spiders. J Geophys Res, Planets 108. https://doi.org/10.1029/2002JE002007

Piqueux S, Kleinböhl A, Hayne PO, Kass DM, Schofield JT, McCleese DJ (2015) Variability of the Martian seasonal CO_2 cap extent over eight Mars years. Icarus 251:164. https://doi.org/10.1016/j.icarus.2014.10.045

Piqueux S, Kleinböhl A, Hayne PO, Heavens NG, Kass DM, McCleese DJ, Schofield JT, Shirley JH (2016) Discovery of a widespread low-latitude diurnal CO_2 frost cycle on Mars. J Geophys Res, Planets 121(7):1174–1189. https://doi.org/10.1002/2016JE005034

Piqueux S, Hayne PO, Kleinböhl A, Kass DM, Schreier M, McCleese DJ, Richardson MI, Schofield JT, Heavens N, Shirley JH (2023) Atmospheric CO_2 depletion near the surface in the Martian polar regions. J Geophys Res, Planets 128:e2022JE007332. https://doi.org/10.1029/2022JE007332

Pommerol A, Schmitt B, Beck P, Brissaud O (2009) Water sorption on Martian regolith analogs: Thermodynamics and near-infrared reflectance spectroscopy. Icarus 114. https://doi.org/10.1016/j.icarus.2009.06.013oi

Pommerol A, Portyankina G, Thomas N, Aye K-M, Hansen CJ, Vincendon M, Langevin Y (2011) Evolution of south seasonal cap during Martian spring: insights from high-resolution observations by HiRISE and CRISM on Mars reconnaissance orbiter. J Geophys Res, Planets 116:E08007. https://doi.org/10.1029/2010JE003790

Pommerol A, Appéré T, Portyankina G, Aye K-M, Thomas N, Hansen CJ (2013) Observations of the northern seasonal polar cap on Mars III: CRISM/HiRISE observations of spring sublimation. Icarus 225:911. https://doi.org/10.1016/j.icarus.2012.08.039

Portyankina G, Markiewicz WJ, Thomas N, Hansen CJ, Milazzo M (2010) HiRISE observations of gas sublimation-driven activity in Mars' southern polar regions: III. Models of processes involving translucent ice. Icarus 205:311.

Portyankina G, Hansen CJ, Aye K-M (2017) Present-day erosion of Martian polar terrain by the seasonal CO_2 jets. Icarus 282:93. https://doi.org/10.1016/j.icarus.2016.09.007

Portyankina G, Merrison J, Iversen JJ, Yoldi Z, Hansen CJ, Aye K-M, Pommerol A, Thomas N (2019) Laboratory investigations of the physical state of CO_2 ice in a simulated Martian environment. Icarus 322:210. https://doi.org/10.1016/j.icarus.2018.04.021

Portyankina G, Hansen CJ, Aye K-M (2020) How Martian araneiforms get their shapes: morphological analysis and diffusion-limited aggregation model for polar surface erosion. Icarus 342:113217. https://doi.org/10.1016/j.icarus.2019.02.032

Poulet F, Langevin Y, Boubin G, Jouglet D, Bibring J-P, Gondet B (2008) Spectral variability of the Martian high latitude surfaces. Geophys Res Lett: L20201. https://doi.org/10.1029/2008GL035450oi

Prettyman TH, Feldman WC, Titus TN (2009) Characterization of Mars' seasonal caps using neutron spectroscopy. J Geophys Res, Planets 114:E08005. https://doi.org/10.1029/2008JE003275

Putzig NE, Phillips RJ, Campbell BA, Holt JW, Plaut JJ, Carter LM, Egan AF, Bernardini F, Safaeinili A, Seu R (2009) Subsurface structure of planum boreum from Mars reconnaissance orbiter shallow radar soundings. Icarus 204:443. https://doi.org/10.1016/j.icarus.2009.07.034

Raack J, Reiss D, Appéré T, Vincendon M, Ruesch O, Hiesinger H (2015) Present-day seasonal gully activity in a south polar pit (Sisyphi Cavi) on Mars. Icarus 251:226. https://doi.org/10.1016/j.icarus.2014.03.040

Rangarajan VG, Tornabene LL, Osinski GR, Conway SJ, Seelos FP, Silvestro S, Salese F, Pajola M, Lucchetti A, Munaretto G, Bickel VT, Thomas N, Cremonese G (2023) Change detection and monitoring of active Martian surface phenomena with the Colour and Stereo Surface Imaging System (CaSSIS) onboard the ExoMars Trace Gas Orbiter (TGO). Icarus 394:115443. https://doi.org/10.1016/j.icarus.2023.115443

Reiss D, Jaumann R (2003) Recent debris flows on Mars: Seasonal observations of Russell Crater dune field. Geophys Res Lett 30:1321. https://doi.org/10.1029/2002GL016704

Reiss D, Erkeling G, Bauch KE, Hiesinger H (2010) Evidence for present day gully activity on the Russell crater dune field. Mars Geophys Res Lett 37:L06203. https://doi.org/10.1029/2009gl042192

Reiss D, Raack J, Hiesinger H (2011) Bright dust devil tracks on Earth: implications for their formation on Mars. Icarus 211(1):917–920. https://doi.org/10.1016/j.icarus.2010.09.009

Reiss D, Zimmerman MI, Lewellen DC (2013) Formation of cycloidal dust devil tracks by redeposition of coarse sands in southern Peru: implications for Mars. Earth Planet Sci Lett 383:7–15. https://doi.org/10.1016/j.epsl.2013.09.033

Reiss D, Spiga A, Erkeling G (2014) The horizontal motion of dust devils on Mars derived from CRISM and CTX/HiRISE observations. Icarus 227:8. https://doi.org/10.1016/j.icarus.2013.08.028

Reiss D, Fenton L, Neakrase L, Zimmerman M, Statella T, Whelley P, Rossi AP, Balme M (2016) Dust devil tracks. Space Sci Rev 203:143. https://doi.org/10.1007/s11214-016-0308-6

Russell P, Thomas N, Byrne S, Herkenhoff K, Fishbaugh K, Bridges N, Okubo C, Milazzo M, Daubar I, Hansen C, McEwen A (2008) Seasonally active frost-dust avalanches on a North polar scarp of Mars captured by HiRISE. Geophys Res Lett 35:L23204. https://doi.org/10.1029/2008GL035790

Russell PS, Byrne S, Pathare A, Herkenhoff KE (2012) Active erosion and evolution of Mars North polar scarps. In: 43rd Annual Lunar and Planetary Science Conference, p 2747

Schaefer EI, McEwen AS, Sutton SS (2019) A case study of recurring slope lineae (RSL) at Tivat crater: implications for RSL origins. Icarus 317:621. https://doi.org/10.1016/j.icarus.2018.07.014

Schmidt F, Douté S, Schmitt B, Vincendon M, Bibring J-P, Langevin Y, Omega Team (2009) Albedo control of seasonal south polar cap recession on Mars. Icarus 200:374.

Schmidt F, Schmitt B, Douté S, Forget F, Jian J-J, Martin P, Langevin Y, Bibring J-P, OMEGA Team (2010) Sublimation of the Martian CO_2 seasonal south polar cap. Planet Space Sci 58:1129. https://doi.org/10.1016/j.pss.2010.03.018

Schmidt F, Andrieu F, Costard F, Kocifaj M, Meresescu A (2017) Formation of recurring slope lineae on Mars by rarefied gas-triggered granular flows. Nat Geosci 10:270–273. https://doi.org/10.1038/ngeo2917

Schorghofer N, Edgett KS (2006) Seasonal surface frost at low latitudes on Mars. Icarus 180(2):321–334. https://doi.org/10.1016/j.icarus.2005.08.022

Schorghofer N, Aharonson O, Khatiwala S (2002) Slope streaks on Mars: correlations with surface properties and the potential role of water. Geophys Res Lett 29(23):41–44. https://doi.org/10.1029/2002GL015889

Schorghofer N, Aharonson O, Gerstell MF, Tatsumi L (2007) Three decades of slope streak activity on Mars. Icarus 191(1):132–140. https://doi.org/10.1016/j.icarus.2007.04.026

Seu R, Phillips RJ, Biccari D, Orosei R, Masdea A, Picardi G, Safaeinili A, Campbell BA, Plaut JJ, Marinangeli L, Smrekar SE, Nunes DC (2007) SHARAD sounding radar on the Mars reconnaissance orbiter. J Geophys Res, Planets 112:E05S05. https://doi.org/10.1029/2006JE002745

Silvestro S, Fenton LK, Vaz DA, Bridges NT, Ori GG (2010) Ripple migration and dune activity on Mars: evidence for dynamic wind processes. Geophys Res Lett 37:20203

Silvestro S, Vaz DA, Fenton LK, Geissler PE (2011) Active aeolian processes on Mars: a regional study in Arabia and meridiani terrae. Geophys Res Lett 38:20201

Silvestro S, Vaz DA, Ewing RC, Rossi AP, Fenton LK, Michaels TI, Flahaut J, Geissler PE (2013) Pervasive aeolian activity along rover Curiosity's traverse in Gale crater. Mars Geol. https://doi.org/10.1130/g34162.1

Silvestro S, Chojnacki M, Vaz DA, Cardinale M, Yizhaq H, Esposito F (2020) Megaripple migration on Mars. J Geophys Res 125:e2020JE006446. https://doi.org/10.1029/2020je006446

Smith IB, Hayne PO, Byrne S, Becerra P, Kahre M, Calvin W, Hvidberg C, Milkovich S, Buhler P, Landis M, Horgan B, Kleinböhl A, Perry MR, Obbard R, Stern J, Piqueux S, Thomas N, Zacny K, Carter L, Edgar L, Emmett J, Navarro T, Hanley J, Koutnik M, Putzig N, Henderson BL, Holt JW, Ehlmann B, Parra S, Lalich D, Hansen C, Hecht M, Banfield D, Herkenhoff K, Paige DA, Skidmore M, Staehle RL, Siegler M (2020) The holy grail: a road map for unlocking the climate record stored within Mars' polar layered deposits. Planet Space Sci 184:104841. https://doi.org/10.1016/j.pss.2020.104841

Smith IB, Calvin W, Becerra P, Landis M, Byrne S, Hayne P, Bapst J, Chmielewski AB, Delaune J (2022) Bifrost: Mars polar science enabled by a low-cost helicopter, at low-cost science mission concepts for Mars exploration. LPI Contrib 2655:5066.

Stanzel C, Pätzold M, Williams DA, Whelley PL, Greeley R, Neukum G, HRSC Co-Investigator Team (2008) Dust devil speeds, directions of motion and general characteristics observed by the Mars Express high resolution stereo camera. Icarus 197:39. https://doi.org/10.1016/j.icarus.2008.04.017

Stcherbinine A, Vincendon M, Montmessin F, Beck P (2021) Identification of a new spectral signature at 3 μm over Martian northern high latitudes: implications for surface composition. Icarus 369:114627. https://doi.org/10.1016/j.icarus.2021.114627

Stillman DE, Michaels TI, Grimm RE, Hanley J (2016) Observations and modeling of northern mid-latitude recurring slope lineae (RSL) suggest recharge by a present-day Martian briny aquifer. Icarus 265:125–138. https://doi.org/10.1016/j.icarus.2015.10.007

Stillman DE, Michaels TI, Hoover RH, Barth EL, Primm KM, Egan AF, Grimm RE (2021) Evaluation of grainflow mechanisms for Martian recurring slope lineae (RSL). Icarus 369:114648

Su S, Fanara L, Zhang X, Hauber E, Gwinner K, Oberst J (2023) Searching for the sources of ice block falls at the Martian North polar scarps. Icarus 390:115321. https://doi.org/10.1016/j.icarus.2022.115321

Sullivan R, Thomas P, Veverka J, Malin M, Edgett KS (2001) Mass movement slope streaks imaged by the Mars Orbiter Camera. J Geophys Res, Planets 106(E10):23607–23633. https://doi.org/10.1029/2000je001296

Sullivan R, Arvidson R, Bell JF, Gellert R, Golombek M, Greeley R, Herkenhoff K, Johnson J, Thompson S, Whelley P, Wray J (2008) Wind-driven particle mobility on Mars: Insights from Mars Exploration Rover observations at "El Dorado" and surroundings at Gusev Crater. J Geophys Res, Planets 113. https://doi.org/10.1029/2008JE003101

Tanaka KL, Scott DH (1987). USGS Map I-1802-C

Thomas PC, Malin MC, Edgett KS, Carr MH, Hartmann WK, Ingersoll AP, James PB, Soderblom LA, Veverka J, Sullivan R (2000) North-south geological differences between the residual polar caps on Mars. Nature 404:161. https://doi.org/10.1038/35004528

Thomas N, Hansen CJ, Portyankina G, Russell PS (2010) HiRISE observations of gas sublimation-driven activity in Mars' southern polar regions: II. Surficial deposits and their origins. Icarus 205:296.

Thomas N, Portyankina G, Hansen CJ, Pommerol A (2011) HiRISE observations of gas sublimation-driven activity in Mars' southern polar regions: IV. Fluid dynamics models of CO_2 jets. Icarus 212:66–85. https://doi.org/10.1016/j.icarus.2010.12.016

Thomas N, 60 colleagues (2017) The Colour and Stereo Surface Imaging System (CaSSIS) for the ExoMars Trace Gas Orbiter. Space Sci Rev 212:1897. https://doi.org/10.1007/s11214-017-0421-1

Tornabene LL, Seelos FP, Pommerol A, Thomas N, Caudill CM, Becerra P, Bridges JC, Byrne S, Cardinale M, Chojnacki M, Conway SJ, Cremonese G, Dundas CM, El-Maarry MR, Fernando J, Hansen CJ, Hansen K, Harrison TN, Henson R, Marinangeli L, McEwen AS, Pajola M, Sutton SS, Wray JJ (2017) Image simulation and assessment of the colour and spatial capabilities of the Colour and Stereo Surface Imaging System (CaSSIS) on the ExoMars Trace Gas Orbiter. Space Sci Rev 214:18. https://doi.org/10.1007/s11214-017-0436-7

Vago J, Witasse O, Svedhem H, Baglioni P, Haldemann A, Gianfiglio G, Blancquaert T, McCoy D, de Groot R (2015) ESA ExoMars program: the next step in exploring Mars. Sol Syst Res 49:518. https://doi.org/10.1134/S0038094615070199

Valantinas A, Becerra P, Pommerol A, Tornabene LL, Affolter L, Cremonese G, et al (2021) CaSSIS color and multi-angular observations of Martian slope streaks. Planet Space Sci 209:105373. https://doi.org/10.1016/j.pss.2021.105373

Valantinas A, Thomas N, Pommerol A, et al (2024) Evidence for transient morning water frost deposits on the Tharsis volcanoes of Mars. Nat Geosci 17:608–616. https://doi.org/10.1038/s41561-024-01457-7

Vandaele AC, 52 colleagues (2018) NOMAD, an integrated suite of three spectrometers for the ExoMars trace gas mission: technical description, science objectives and expected performance. Space Sci Rev 214:80. https://doi.org/10.1007/s11214-018-0517-2

Verba CA, Geissler PE, Titus TN, Waller D (2010) Observations from the High Resolution Imaging Science Experiment (HiRISE): Martian dust devils in Gusev and Russell craters. J Geophys Res, Planets 115. https://doi.org/10.1029/2009JE003498

Vincendon M, Mustard J, Forget F, Kreslavsky M, Spiga A, Murchie S, Bibring J-P (2010) Near-tropical subsurface ice on Mars. Geophys Res Lett 37(1). https://doi.org/10.1029/2009GL041426

Vincendon M, Pilorget C, Carter J, Stcherbinine A (2019) Observational evidence for a dry dust-wind origin of Mars seasonal dark flows. Icarus 325:115–127. https://doi.org/10.1016/j.icarus.2019.02.024

Wellington DF, Bell JF (2020) Patterns of surface albedo changes from Mars reconnaissance orbiter Mars color imager (MARCI) observations. Icarus 349:113766. https://doi.org/10.1016/j.icarus.2020.113766

Wells EN, Veverka J, Thomas P (1984) Mars: experimental study of albedo changes caused by dust fallout. Icarus 58(3):331–338. https://doi.org/10.1016/0019-1035(84)90079-4

Williams SH (1991) Dark Talus Streaks on Mars are Similar to Aeolian Dark Streaks. In: Lunar and Planetary Science Conference XXII, p 1509

Witten TA, Sander LM (1983) Diffusion-limited aggregation. Phys Rev B 27(9)

Xiao H, Stark A, Schmidt F, Hao J, Steinbrügge G, Wagner NL, Su S, Cheng Y, Oberst J (2022a) Spatio-temporal level variations of the Martian seasonal North polar cap from co-registration of MOLA profiles. J Geophys Res, Planets 127:e2021JE007158. https://doi.org/10.1029/2021JE007158

Xiao H, Stark A, Steinbrügge G, Thor R, Schmidt F, Oberst J (2022b) Prospects for mapping temporal height variations of the seasonal CO_2 snow/ice caps at the Martian poles by co-registration of MOLA profiles. Planet Space Sci 214:105446. https://doi.org/10.1016/j.pss.2022.105446

Zhang L, Li YR, Zhou LQ, Wu CM (2017) Comparison study on the calculation formula of evaporation mass flux through the plane vapour-liquid interface. J Phys Conf Ser 925:012019. https://doi.org/10.1088/1742-6596/925/1/012019

Zhao Y, Zhong L, Yuan R, Zhao C, Li R, Wang Y, Lian Y, Richardson M (2021) Simulation of Martian dust effects on polar CO_2 ice caps and atmospheric circulation using the MarsWRF model. J Geophys Res, Planets 126:e06937. https://doi.org/10.1029/2021JE006937

Zurek RW, Smrekar SE (2007) An overview of the Mars Reconnaissance Orbiter (MRO) science mission. J Geophys Res, Planets 112:E05S01. https://doi.org/10.1029/2006JE002701

Zurek RW, Barnes JR, Haberle RM, Pollack JB, Tillman JE, Leovy CB (1992) Dynamics of the atmosphere of Mars. In: Kieffer HH, Jakosky BM, Snyder CW, Matthews MS (eds) Mars (A93-27852 09-91). Univ. Arizona Press, p 835

Zurek RW, Bougher SW, Tolson R, Baird D, Demcak S, Kass DM, Lugo R, Jakosky BM (2018) The 2018 planet-encircling dust storm: effects on the Mars upper atmosphere as seen in MAVEN accelerometer data. AGU Fall Meet Abstr 2018:P43J-3864